

December 2020

## Fabrication of Binder-Free Electrodes Based on Graphene Oxide with CNT for Decrease of Resistance

Di Zhang  
*University of Massachusetts Amherst*

Follow this and additional works at: [https://scholarworks.umass.edu/masters\\_theses\\_2](https://scholarworks.umass.edu/masters_theses_2)



Part of the [Other Mechanical Engineering Commons](#)

---

### Recommended Citation

Zhang, Di, "Fabrication of Binder-Free Electrodes Based on Graphene Oxide with CNT for Decrease of Resistance" (2020). *Masters Theses*. 1002.

<https://doi.org/10.7275/18550008> [https://scholarworks.umass.edu/masters\\_theses\\_2/1002](https://scholarworks.umass.edu/masters_theses_2/1002)

This Open Access Thesis is brought to you for free and open access by the Dissertations and Theses at ScholarWorks@UMass Amherst. It has been accepted for inclusion in Masters Theses by an authorized administrator of ScholarWorks@UMass Amherst. For more information, please contact [scholarworks@library.umass.edu](mailto:scholarworks@library.umass.edu).

**FABRICATION OF BINDER-FREE ELECTRODES BASED ON GRAPHENE  
OXIDE/CNT FOR DECREASE OF RESISTANCE**

A Thesis Presented

by

DI ZHANG

Submitted to the Graduate School of the  
University of Massachusetts Amherst in partial fulfillment  
of the requirements for the degree of

MASTER OF SCIENCE IN MECHANICAL ENGINEERING

September 2020

Mechanical and Industrial Engineering

© Copyright by Di Zhang 2020

All Rights Reserved

**FABRICATION OF BINDER-FREE ELECTRODES BASED ON GRAPHENE  
OXIDE/CNT FOR DECREASE OF RESISTANCE**

A Thesis Presented

by

DI ZHANG

Approved as to style and content by:

---

Byung H. Kim, Chair

---

Yanfei Xu, Member

---

Dimitrios Maroudas, Member

---

Sundar Krishnamurty, Department Head  
Mechanical and Industrial Engineering

## DEDICATION

*To,*

*My Parents,*

*For encouraging and gave me a strong soul*

*My Grandfather,*

*For his endless love*

## ACKNOWLEDGMENTS

First, I would like to thank my principal advisor, Professor Byung Kim, for his reliance, guidance, and support. I would not have been able to complete and write this thesis without your invaluable assistance. Thank you for being a life mentor by teaching me the importance of hard work and discipline on the road to self-improvement. I would not have been able to find the goal of my life without your support.

I would like to thank the members of my thesis committee. A very special thanks to Professor Yanfei Xu for all the guidance with technical discussions from the beginning of the research. I would also like to thank Professor Dimitrios Maroudas for his guidance in material processing. Without their knowledge and suggestions, this study would not have been successful.

I would also like to express my gratitude to Professor Volodymyr Duzhko, Professor Alexander Ribbe, Professor James Watkins, and his student Wenhao Li, as well as Huafeng Fei. I am very thankful for their expertise and assistance with this project.

I am also very grateful to my colleagues Jeonhyeong Yeo and Nariman Banaei. Their assistance with the SEM analysis and other lab equipment was very helpful throughout the project.

Furthermore, I would like to thank the University of Massachusetts Amherst for providing a comfortable research environment and facilities while I completed this project.

## ABSTRACT

### FABRICATION OF BINDER-FREE ELECTRODES BASED ON GRAPHENE OXIDE/CNT FOR DECREASE OF RESISTANCE

SEPTEMBER 2020

DI ZHANG

B.S., UNIVERSITY OF MASSACHUSETTS AMHERST

M.S.M.E., UNIVERSITY OF MASSACHUSETTS AMHERST

Directed by: Professor Byung H. Kim

In electrode double layer capacitor (EDLC), electrodes usually contain binder materials to provide adhesion between electrode materials. However, binder materials usually bring unwanted resistances to the component due to their non-conductivity properties and the occupation of ion cavities. The purpose of this thesis is to demonstrate the feasibility of fabricating electrodes for EDLCs by using carbon nanotubes (CNTs) and graphene oxide (GO) without using any binding materials. At the same time, investigating the binder-free electrode's electrochemical properties and make an assumption of its potential application in the future.

The slurry of binder-free electrodes was fabricated by ultrasonically suspending CNTs and GO aqueous solution. The ultrasonicated mixture was then casted on an aluminum foil, followed by drying processes to form into an electrode film. By combining the CNTs/GO binder-free electrodes with aqueous electrolyte, a symmetrical electrode double layer capacitor (EDLC) was fabricated. The EDLC was also tested for electrochemical performance using a polyvinyl alcohol (PVA) based gel electrolyte. It was found that an electrode with a low resistance was achieved by eliminating the use of binders. The as-prepared sample had an equivalent series resistance (ESR) of 0.07 Ohms. Furthermore, a solid-state, binder-free EDLC sample achieved a specific capacitance of 0.2876 F/m<sup>2</sup> in volumetric terms, or 58.24 mF/g in gravimetric terms.

The laboratorial investigation demonstrates a possible scheme of decreasing resistance start with eliminating binding materials in electrodes. Successfully fabricated binder-free electrodes show the feasibility of eliminating binding materials in electrodes. The easy access fabrication process of graphene oxide/CNT electrodes provides a chance for mass production in the industry. Solid-state electrolyte samples also give an example of making all-solid-state energy storage devices.



## TABLE OF CONTENTS

	Page
ACKNOWLEDGMENTS.....	v
ABSTRACT.....	vi
LIST OF TABLES.....	xi
LIST OF FIGURES.....	xii
CHAPTER	
1. INTRODUCTION.....	1
1.1 Thesis Outline.....	1
2. BACKGROUND.....	2
2.1 Introduction.....	2
2.1.1 Supercapacitor Categories.....	3
2.2 Materials and Components .....	4
2.2.1 Carbon .....	4
2.2.2 Carbon-based material.....	4
2.2.3 Electrolyte.....	5
2.3 Applications and Challenges.....	6
2.3.1 Mechanism.....	6
2.3.2 Internal Resistance and Equivalent Series Resistance (ESR).....	7

2.3.3	Temperature .....	8
3.	BINDER-FREE ELECTRODE FABRICATION .....	10
3.1	Background .....	10
3.2	Purpose.....	11
3.3	Preliminary Procedure .....	12
3.4	Experimental Design.....	12
3.4.1	Overview.....	12
3.4.2	Equipment and personal safety equipment .....	13
3.4.3	Carbon Nanotube suspension.....	14
3.4.4	Electrode slurry .....	14
3.5	Aluminum Substrate .....	15
3.6	Casting .....	15
3.7	Surface Checking.....	17
3.7.1	Scanning Electron Microscopy (SEM).....	17
3.8	Results and Discussion .....	19
4.	COMBINING WITH DIFFERENT ELECTROLYTES .....	20
4.1	Purpose.....	20
4.2	Experimental Design.....	20
4.2.1	Equipment and Personal Safety Equipment.....	20
4.2.2	Sulfuric Acid (H <sub>2</sub> SO <sub>4</sub> ).....	21
4.2.3	Gel Electrolyte .....	23
4.2.3.1	Introduction.....	23
4.2.3.2	PVA with H <sub>2</sub> SO <sub>4</sub> .....	24

4.2.3.3 PVA with H <sub>3</sub> PO <sub>4</sub> .....	25
5. TESTING AND RESULTS.....	27
5.1 Method and Equipment.....	27
5.1.1 Cyclic Voltammetry (CV).....	27
5.1.2 Electrochemical Impedance Spectroscopy (EIS).....	29
5.1.2.1 Introduction.....	29
5.1.2.2 Randles Model .....	30
5.2 Results and Analysis.....	31
5.2.1 Obtained GO/CNTs electrodes with the H <sub>2</sub> SO <sub>4</sub> electrolyte.....	31
5.2.2 Obtained GO/CNTs electrodes with the PVA/H <sub>3</sub> PO <sub>4</sub> gel electrolyte.....	33
5.2.3 Obtained GO/CNTs electrodes with the PVA/H <sub>2</sub> SO <sub>4</sub> gel electrolyte.....	35
5.2.4 Maxwell electrode with the PVA/H <sub>3</sub> PO <sub>4</sub> gel electrolyte .....	37
6. CONCLUSION.....	42
7. FUTURE WORK.....	44
7.1 Laser Treatment .....	44
7.2 Electrode Fabrication.....	44
7.3 Electrolyte Fabrication.....	45
7.4 Hybrid Capacitor.....	46
BIBLIOGRAPHY.....	47

## LIST OF TABLES

Table	Page
Table 1: EIS results of all samples.....	42

## LIST OF FIGURES

Figure	Page
Figure 1: Schematic of electrode components. ....	11
Figure 2: Graphene oxide/carbon nanotube dispersion .....	13
Figure 3: Casted GO/CNTs binder-free electrode (5 cm by 5cm).....	16
Figure 4: A picture of the casted GO/CNTs electrode's edge under a microscope. (the top was coated with GO/CNTs material, and the bottom was aluminum foil) .....	17
Figure 5: SEM image of the GO/CNTs electrode surface border. (uncoated aluminum on the left side, GO/CNTs layer on the right side) .....	18
Figure 6: Zoomed in SEM image of the GO/CNTs electrode surface border .....	19
Figure 7: The top two samples were GO/CNTs with an H <sub>2</sub> SO <sub>4</sub> electrolyte, the bottom two samples were GO/CNTs with a PVA/H <sub>3</sub> PO <sub>4</sub> gel electrolyte .....	22
Figure 8: A picture of the PVA/H <sub>2</sub> SO <sub>4</sub> gel electrolyte piece.....	25
Figure 9: A picture of the PVA/H <sub>3</sub> PO <sub>4</sub> gel electrolyte piece.....	26
Figure 10: Schematic of the simplest and most common Randles circuit .....	30
Figure 11: Bode diagram of the obtained GO/CNTs electrode with the H <sub>2</sub> SO <sub>4</sub> electrolyte....	31
Figure 12: Nyquist diagram of the obtained GO/CNTs electrode with the H <sub>2</sub> SO <sub>4</sub> electrolyte.....	32
Figure 13: Open circuit voltage diagram of the obtained GO/CNTs electrode with the H <sub>2</sub> SO <sub>4</sub> electrolyte.....	33
Figure 14: Bode diagram of the obtained GO/CNTs electrode with the PVA/ H <sub>3</sub> PO <sub>4</sub> gel electrolyte.....	34
Figure 15: Nyquist diagram of the obtained GO/CNTs electrode with the PVA/H <sub>3</sub> PO <sub>4</sub> gel electrolyte.....	34

Figure 16: Open circuit voltage diagram of the obtained GO/CNTs electrode with the PVA/ H <sub>3</sub> PO <sub>4</sub> gel electrolyte .....	35
Figure 17: Bode diagram of the obtained GO/CNTs electrode with the PVA/H <sub>2</sub> SO <sub>4</sub> gel electrolyte.....	36
Figure 18: Nyquist diagram of the obtained GO/CNTs electrode with the PVA/H <sub>2</sub> SO <sub>4</sub> gel electrolyte.....	36
Figure 19: Open circuit voltage diagram of the obtained GO/CNTs electrode with the PVA/H <sub>2</sub> SO <sub>4</sub> gel electrolyte .....	37
Figure 20: Bode diagram of the Maxwell electrode with the PVA/H <sub>3</sub> PO <sub>4</sub> gel electrolyte.....	38
Figure 21: Nyquist diagram of the Maxwell electrode with the PVA/H <sub>3</sub> PO <sub>4</sub> gel electrolyte..	39
Figure 22: Open circuit voltage diagram of the Maxwell electrode with the PVA/H <sub>3</sub> PO <sub>4</sub> gel electrolyte.....	39
Figure 23: Cyclic voltammetry diagram of GO/CNTs with the H <sub>2</sub> SO <sub>4</sub> electrolyte. The sample was tested from 0 V to 2 V under a 0.1 V/s scan rate.....	40
Figure 24: Cyclic voltammetry diagram of GO/CNTs with the PVA/H <sub>3</sub> PO <sub>4</sub> gel electrolyte. The sample was tested from 0 V to 2 V under a 0.1 V/s scan rate .....	41
Figure 25: Illustration of a roll-2-roll production line .....	45

## CHAPTER 1

### INTRODUCTION

#### 1.1 Thesis Outline

The objective of this thesis is to demonstrate the feasibility of fabricating binder-free electrodes for EDLCs by using graphene oxide with carbon nanotubes. Investigating the potential of binder-free EDLC for decreasing resistance, developing all-solid-state devices, and mass production.

We begin by exploring the background information of the supercapacitor in the 2<sup>nd</sup> chapter. It contains significant information regarding the basis of this thesis. The topics include the following: the categories of supercapacitors, carbon, and carbon-based material, the electrolyte of energy storage devices, supercapacitor applications and some challenges. In Chapter 3, we explore the fabrication process of the carbon-based electrode without using any binder materials. This chapter also includes details regarding the experimental setup and an overview of the results analysis. Chapter 4 details the different combinations of the binder-free electrodes and electrolytes, including details of the experimental design. Testing results are compared in Chapter 5 primarily through cyclic voltammetry (CV) and electrochemical impedance spectroscopy (EIS). Finally, we describe the conclusions that are drawn from all experiments in Chapter 6, while Chapter 7 describes further manufacturing possibilities that may be attempted in the future.

## CHAPTER 2

### BACKGROUND

#### 2.1 Introduction

As the increased reliance on electricity, the function of storing electrical energy is becoming a crucial problem. For electrical energy storage devices, batteries and capacitors are common options. Rechargeable batteries have been used to store electrical energy in a chemical form, and capacitors have been used to store energy in the form of electrical charge. However, both of them have apparent drawbacks, for example, the low power density and low charging rate of batteries, the low energy density and high self-discharging of capacitors. Therefore, in recent decades, many researchers and scientists have looked toward supercapacitors to overcome these problems. As a branch of supercapacitors, EDLCs filled the gap between batteries and capacitors, are one of the most promising candidates for energy storage for several reasons. [1-6] They have a higher power density than researchable batteries. They also have higher energy density than capacitors, and a longer lifetime when compared to other energy storage devices. However, EDLCs also have drawbacks, leaving much room for improvement.



### 2.1.1 Supercapacitor Categories

Supercapacitors can be described by a number of categories. In the first category, according to interface chemistry and physics, supercapacitors are classified into three major groups. The first group is pseudocapacitors, which rely on redox material to function. The second group is electrical double layer capacitors (EDLCs), which are made of carbon-based materials with a high specific surface area. The last group are hybrid capacitors, which are a combination of an EDLC and an electrochemical pseudocapacitor.

The second category describes the types of supercapacitors based on the electrode material that is used. There are carbon-based electrode supercapacitors, metal oxide electrode supercapacitors, electroconductive polymer capacitors, and compound electrode capacitors, where each capacitor has a different use.

The third category breaks the supercapacitors into groups based on the types of electrolytes used. The supercapacitors are divided into liquid electrolyte supercapacitors, solid electrolyte supercapacitors, and redox-active electrolyte supercapacitors. The liquid electrolyte contains an aqueous electrolyte and a non-aqueous electrolyte. For the aqueous electrolyte, it can be an acidic, alkaline, or neutral solution, and for the non-aqueous electrolyte, it can be an organic solution, an ionic liquid, or a mixture.

## **2.2 Materials and Components**

### **2.2.1 Carbon**

Carbon is a highly stable material that has been widely used in many fields. Its consistent physical and chemical properties ensure reliability when used as electrodes in energy storage devices. The lightweight of carbon also provides portability for devices made with it. In addition, carbon is one of the most abundant materials in the world, which means it has a lower cost when comparing with metallic materials. [7] Furthermore, its non-toxic nature is innocuous to humans and the environment.

### **2.2.2 Carbon-based material**

Most supercapacitors use carbon as a base for electrodes because carbon-based material is a neutral substance with highly porous structures that maximizes the capacity of charge storage. Currently, the most commonly used carbon-based materials for electrodes are active carbon, carbon aerogel, carbon nanotubes, and graphene. [8] Some of the major factors in electrodes that affect the performance of EDLCs are the specific surface area, pore distribution, pore morphology, and functional group. Herein, active carbon is selected because it has a very high specific area, stable physical properties, stable chemical properties, facile processing, and a low cost. These features provide an efficient way to improve the electrochemical performance of EDLCs. However, an average specific capacitance around 100~160 F/g limits its use. [9] Therefore, active carbon is usually processed as active materials in electrodes and combined with other functional groups or posttreatment.

### 2.2.3 Electrolyte

Electrolytes are one of the most essential components for energy storage devices because they determine the electrochemical performance within electrodes when assembled in a supercapacitor. Presently, electrolytes used for supercapacitors are mainly made from either liquid electrolytes, solid electrolytes, or redox-active electrolytes.

An aqueous electrolyte is the most common choice for supercapacitors in research and development due to its advantages of high conductivity, small particle size, high ion concentration, low resistance, and low price. However, it also has various shortcomings. For example, it has a smaller electrochemical window of approximately 1.23 V, low energy density, and weak ion activity at low temperatures. [10]

Organic electrolytes have a wide electrochemical window up to 4 V [11], low levels of corrosion, and a broad range of working temperatures. They also have low conductivity, large ESR, and low performance while they are charging or discharging.

An ionic liquid-based electrolyte provides high thermal, chemical, and electrochemical stability and usually gives operative cell voltages above 3 V. As a result, it is used as an electrolyte additive due to its high viscosity and high cost. [10]

Using solid electrolytes eliminate both the use of a separator and the hazards of leakage. The crystal structure of the solid electrolyte is beneficial to the transfer of ions and gives the device a large temperature range. However, poor electrolyte dissolution and low electrical conductivity limit its applications in the battery and supercapacitor industry.

## 2.3 Applications and Challenges

### 2.3.1 Mechanism

Supercapacitor use has increased around the world due to its valuable working mechanisms. They have been used in electronic devices, automobiles, buses, solar and wind power systems, and many other fields that require rapid charge and discharge cycles rather than long-term energy storage. To better understand the pros and cons of supercapacitors, the mechanism of supercapacitor is discussed here.

As far as pseudocapacitors are concerned, electron charges come from a desolvated and adsorbed ion; only one electron per charge unit participates during the charge transfer process, which occurs between the electrolyte and electrodes [12]. When a potential difference is applied, ions in the electrolyte diffuse to electrodes and enter the surface active oxide through electrochemical reactions. This faradaic charge transfer originates from a sequence of reversible faradaic redox, electrosorption or intercalation processes on the electrode surface.

However, the mechanism of EDLCs is different than that of pseudocapacitors. During the charging and discharging period of EDLCs, ions move across the separator to the electrode and are absorbed into their porous structure. Therefore, EDLCs have no chemical reactions during the charging or discharging period. The capacitance is produced by electrostatic charge separation at the interface between the electrode and the electrolyte [10]. In other words, when a potential difference is applied to an EDLC, the charge will be directly stored through an electrostatic field, which is purely a physical process. Due to this feature, EDLCs have an inherently faster charging and discharging capacity. This feature also ensures that the electrodes and electrolyte hardly age or decay,

giving EDLCs a million-cycle lifetime and a larger power density when compared to those of rechargeable batteries.

During the charging and discharging process, some ions are lost due to movement, which is known as resistance. Ions lost over time by vaporization and diffusion causes a reduction in conducting materials and reduces the contact area [13]. Supercapacitors with a high number of lost ions have a high resistance. Therefore, it is important to eliminate the resistance to improve the ion storage ability. More details are discussed in the next section.

### **2.3.2 Internal Resistance and Equivalent Series Resistance (ESR)**

The internal resistance and equivalent series resistance (ESR) of supercapacitors are mainly made up of the electrode material resistance, electrolyte resistance, and contact resistance. It is important to evaluate the ESR of the energy storage device because it is related to energy loss, heat generation, and power density.

To make the analysis evident and more straightforward, supercapacitors are treated as three electrical components: an internal resistor, an external resistor, and a capacitor. They are either in parallel or series and connected as a resistor/capacitor (RC) circuit model. When a direct current (DC) is applied, according to Ohm's law, the internal resistance  $R$  is calculated from the potential difference ( $V_1, V_2$ ) during the charging or discharging process at a certain time with a constant current flow  $I$ . This gives a better understanding of the calculation, and the resistance can be calculated by the following equation:

$$R = \frac{V_2 - V_1}{I}$$

With alternating current (AC), which periodically reverses directions, the maximum current delivered by the supercapacitor is directly dependent on its internal resistance and ESR. The current passing through the ESR reduces the voltage  $V$  of the supercapacitor by the resistance  $R$  multiplied by the loading current  $I$  [14]:

$$V = I * R$$

Furthermore, the current flowing through the ESR consumes the output power due to a relationship between power ( $P$ ) and resistance:

$$P = I^2 * R$$

Consequently, a supercapacitor or other energy storage device needs to have a low internal resistance and ESR to increase the power output if the current is required to be a steady variable.

### 2.3.3 Temperature

A liquid electrolyte is normally very sensitive to the temperature in supercapacitors. Organic electrolytes may react with oxygen that is present in the air due to unstable chemical components that it contains. Aqueous electrolytes usually have a narrow potential window and working temperature range. For these reasons, solid-state electrolytes have an advantage over others in this aspect. Nowadays, more and more scientists and researches are putting effort in studying solid-state energy storage devices.

The ESR is mainly affected by the viscosity of the electrolyte. However, the viscosity of a liquid electrolyte is mainly affected by temperature. The ion activity of a liquid electrolyte decreases significantly when the environmental temperature is lower than a certain degree (usually around negative 20 degrees Celsius). [15] Therefore, a wide range of working temperatures for energy storage devices provides more convenience in applications and removes the limitation of their electrochemical performance under low temperature/ conditions.

## CHAPTER 3

### BINDER-FREE ELECTRODE FABRICATION

#### 3.1 Background

The focus of Chapter 3 is on Huang's contribution to a binder-free electrode, which assists in eliminating the use of binder in EDLCs. The experiment in this study was designed according to the work of Huang [16].

In an energy storage device, the electrode is one of the most important parts that determines the electrochemical performance. For the components of the electrode, the binder is significant in the intermediate design between the active materials and the current collector (substrate). However, the binder is usually made of nonconductive materials, which occupy ion cavities in the electrodes and bring unwanted resistance. As a result, the use of binder materials always lowers the electrochemical performance of the device. (Figure 1)



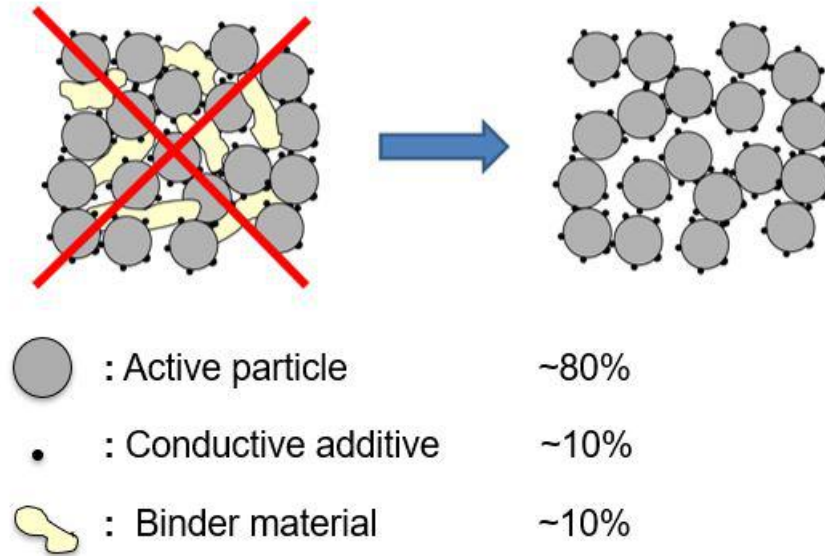


Figure 1: Schematic of electrode components [17].

### 3.2 Purpose

Electrodes are mainly made of active materials (for example, active carbon) because they have a great electrical conductivity and provide a large specific area for storing ions at the same time. To improve the thermal and electrical conductivity, conductive additives (for example, metal alloy powders) can be added. To combine the active and additive materials and stick them onto a current collector, a binder is needed to provide adhesion forces. The binder material used in an electrode is usually made of nonconductive material, and the use of this material negatively impacts the electrical conductivity due to its nonconductive property. Thus, eliminating the binder in electrodes is a significant step in improving the performance of energy storage devices. The purpose of this experiment is to prove the feasibility of producing binder-free electrodes through a facile method and then testing the electrochemical performance of the obtained electrode.

### 3.3 Preliminary Procedure

Based on Huang and his team's work [16], the process of making binder-free electrodes for energy storage devices was reviewed and modified. The procedure of creating a binder-free electrode involves a purely physical process that includes stable and nontoxic raw materials. These materials are fabricated under a highly controllable process involving ultrasonication. The entire procedure is completed quickly compared to that of chemical processes, such as chemical vapor deposition [18, 19]. Reducing the number of steps in the procedure can increase the production efficiency and decrease the fabrication cost at the same time.

### 3.4 Experimental Design

#### 3.4.1 Overview

For this experiment, several steps were taken to build a binder-free electrode. The amphiphilic nature of graphene oxide (GO) allowed for the adsorption of carbon nanotubes (CNTs) onto their surface in water, which formed a highly stable dispersion [20]. The GO/CNTs hybrid electrode films then self-assembled on a substrate via a simple casting of an aqueous dispersion. This method provided a great opportunity to assemble a binder-free electrode for supercapacitors. Due to negative impacts from binder materials, the electrode created without binder materials had reduced resistance and increased charge transfer efficiency.

The GO/CNTs aqueous dispersion, as shown in Figure 2, was synthesized through a full physical process and therefore did not contain any chemical reactions. A 20% (in weight) CNT solution was made. First, the CNTs were mixed with deionized water in an

ultrasonic bath. After ultrasonication for 2 hours, a probe ultrasonication process was applied for 10 minutes. Then, the CNT solution was mixed with the prepared GO solution (1 mg/ml) in an ultrasonic bath for 10 minutes.

Finally, the resulting GO/CNTs mixture was directly cast on a substrate to form a binder-free electrode film [21].

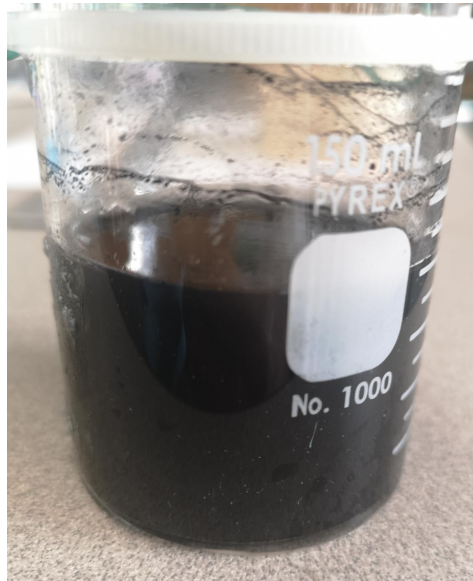


Figure 2: Graphene oxide/carbon nanotube dispersion.

### 3.4.2 Equipment and personal safety equipment

Equipment:

- Ultrasonic bath
- Hotplate with magnetic stirring
- Scale and weigh paper
- DC power supply
- Stainless steel mixing paddle

- 2 x 200-mL glass beaker
- Plastic dropper
- 10-mL measuring cylinder

Safety equipment:

- Long sleeved lab coat
- Safety goggles
- Powderless plastic gloves
- 3M half-mask respirator

### **3.4.3 Carbon Nanotube suspension**

Short-length single-walled carbon nanotubes (CNTs) (US4130, US Research Nanomaterials) were used without functionalization. The 20% carbon nanotube suspension was prepared by adding 20 mg CNTs into 80 mL distilled water and sonicating in an ultrasonic bath for 2 hours, followed by probe ultrasonication for 10 minutes.

It is notable that, the CNT dispersion was unstable because the CNTs reaggregated immediately after ultrasonication because of their hydrophobic nature. Therefore, the dispersion was mixed with graphene oxide once it was obtained.

### **3.4.4 Electrode slurry**

A 1 ml monolayer graphene oxide water dispersion (4 mg/ml) was purchased from MSE Supplies (MSE19A92800V) and diluted to 1 mg/ml before use.

To fabricate the electrode slurry, 20 mL of prepared graphene oxide aqueous dispersion was added at a concentration of 1 mg/mL to the obtained CNT dispersion. The

mixture was sonicated in an ultrasonic bath for 10 minutes to obtain a highly stable GO/CNTs hybrid aqueous dispersion. The obtained slurry was directly used for casting on the substrate to fabricate electrodes.

### **3.5 Aluminum Substrate**

Here, aluminum foil was chosen to be used as substrate instead of Huang's Titanium alloy for several reasons. Aluminum has a higher electric conductivity than titanium; it can be easier processed in the laboratory; and it has a lower price. A pure 1100 aluminum foil offering a superior electrical conductivity; it was purchased from McMaster-Carr and used directly. The foil was cut into a 6 cm square. It was then applied to a square glass plate (5 cm length, 2 mm thickness) to make a flat coating surface (with a 5\*5 cm<sup>2</sup> valid coating area).

### **3.6 Casting**

A binder-free electrode was produced by casting the electrode slurry onto the prepared aluminum substrate with a hotplate at 180 degrees Celsius. When the GO/CNTs dispersion was dropped on the substrate, water evaporation occurred. The formed GO/CNTs film on the aluminum substrate was the electrode material, as shown in the figure below. For a 5 cm by 5 cm substrate, each electrode had 10 mL dispersion dropped on its surface.

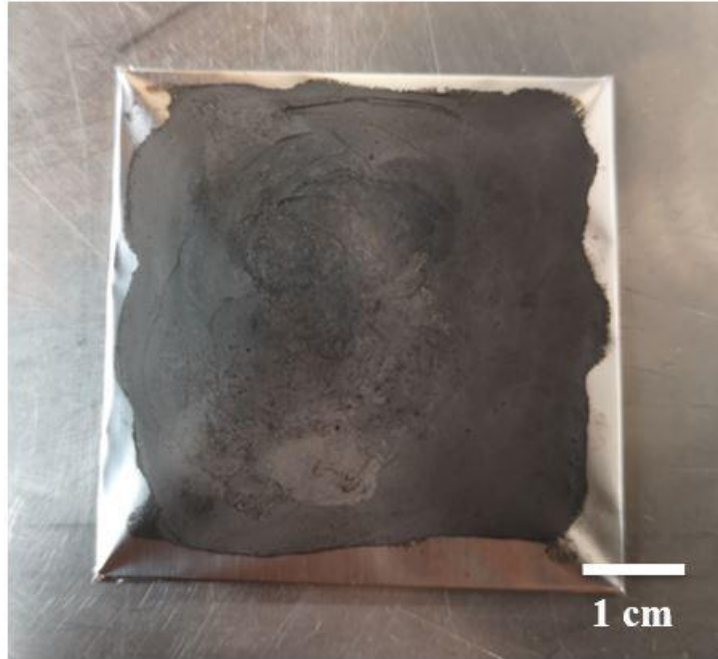


Figure 3: Casted GO/CNTs binder-free electrode (5 cm by 5 cm).

It is noticeable that, due to the electrode slurry was manually dropped on the substrate, and the aluminum foil was deformed during the water evaporating process. The valid casted area was smaller than  $25 \text{ cm}^2$ , which also means the area for charge transfer was also smaller. The casting process can be improved by using a roll-2-roll process. The electrode material can be casted much more evenly distributed, and the electrode film can be fabricated much faster through a manufacturing tool like roll-2-roll. More details are discussed in Chapter 7.

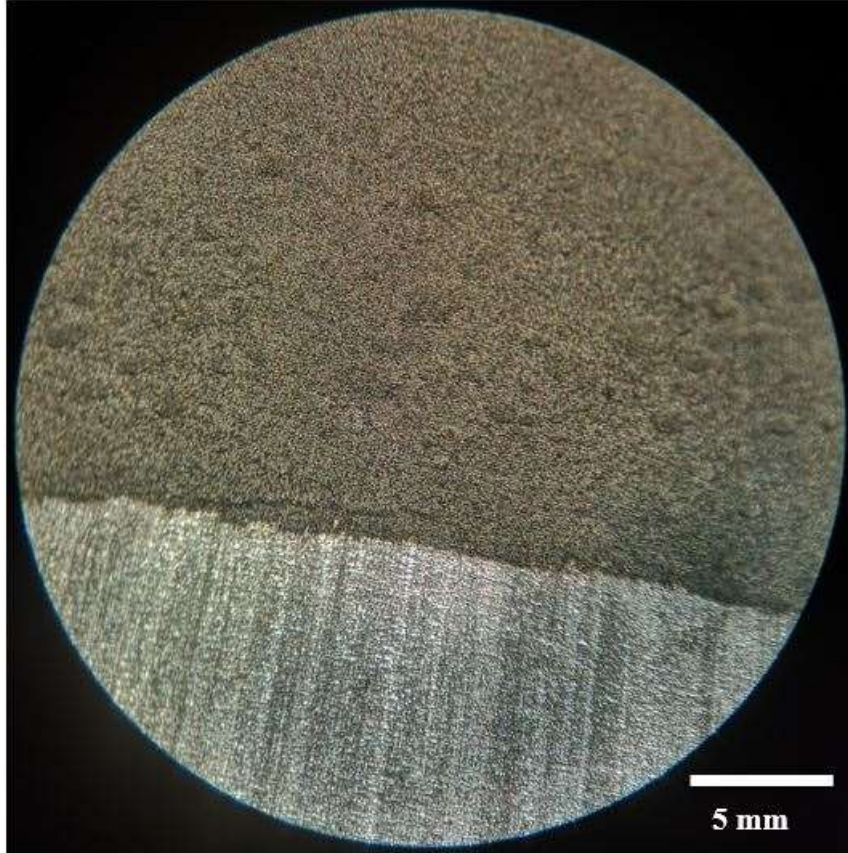


Figure 4: A picture of the casted GO/CNTs electrode's edge under a microscope. (the top was coated with GO/CNTs material, and the bottom was aluminum foil)

### 3.7 Surface Checking

#### 3.7.1 Scanning Electron Microscope (SEM)

Scanning electron microscopy (SEM) is a widely used tool for investigating the microstructure of materials. It can produce images of a sample by scanning its surface through a focused beam of electrons [22]. To check the effect of casting, an SEM technique was applied to an obtained GO/CNTs electrode sample. From the image below,

the casted substrate had a more rugged surface, which was obviously different from the uncoated surface.

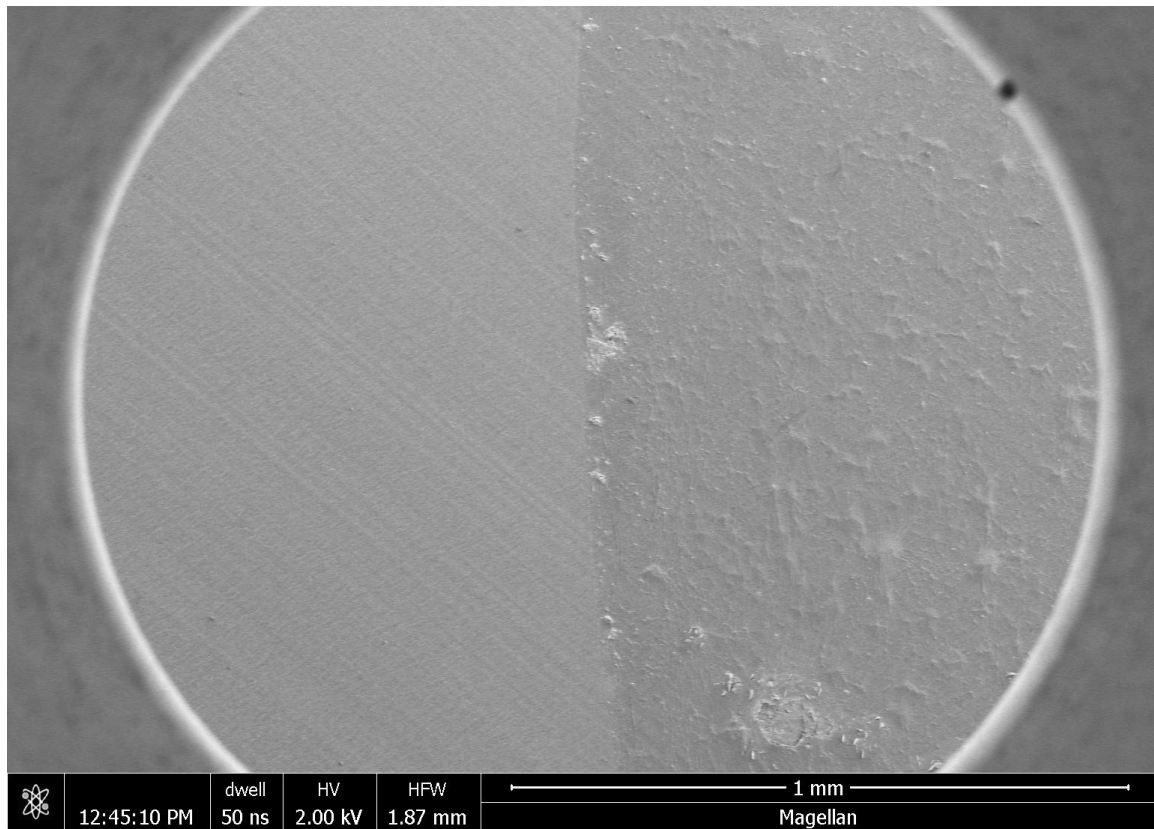


Figure 5: SEM image of the GO/CNTs electrode surface border. (uncoated aluminum on the left side, GO/CNTs layer on the right side)



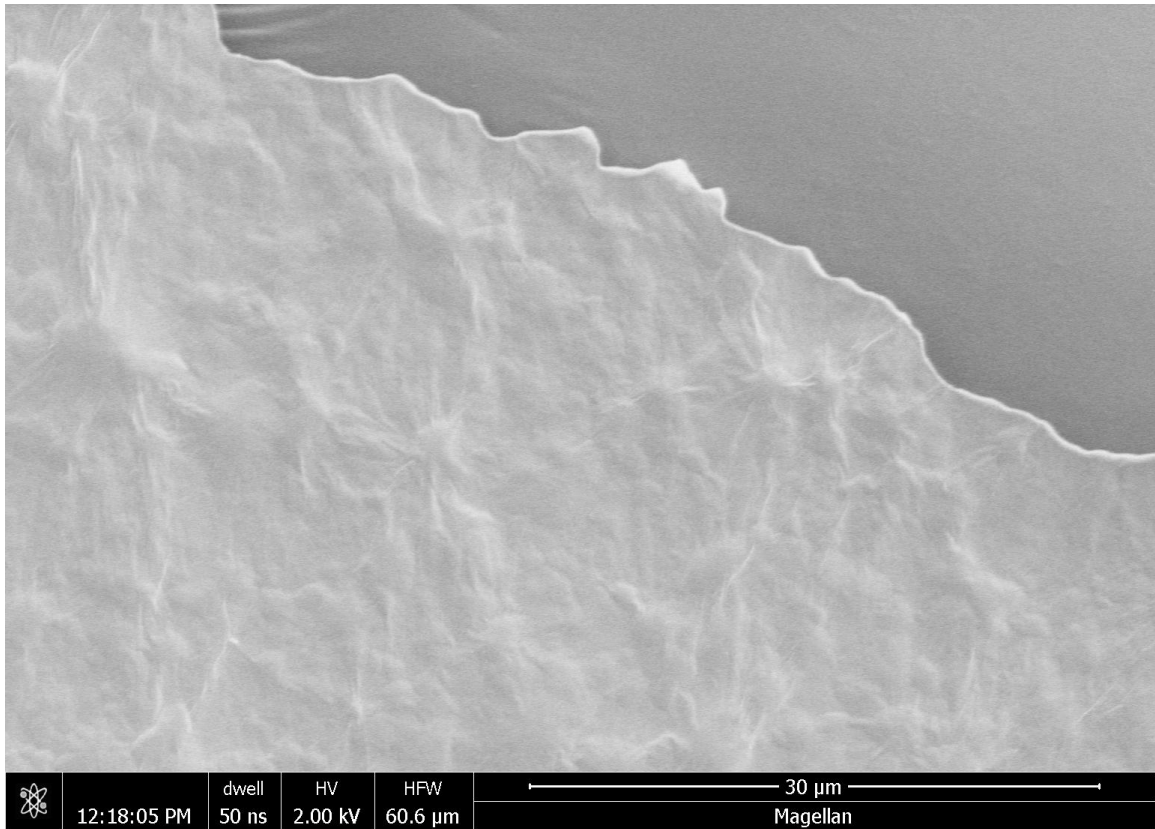


Figure 6: Zoomed in SEM image of the GO/CNTs electrode surface border.

### 3.8 Results and Discussion

Based on the SEM results, it is clearly shown that the GO/CNTs surface was coated on the aluminum foil. Before casting, the aluminum foil had a smooth and clear surface. After electrode casting, the casted area became rough and thicker. From the observed result in Figure 5 and 6, we inferred that the GO/CNTs electrode can be casted on the aluminum surface without using any binding materials. Therefore, there was no binder used when making electrode, and no binding material used between electrode layer and substrate.

## CHAPTER 4

### COMBINING WITH DIFFERENT ELECTROLYTES

#### 4.1 Purpose

For energy storage devices such as EDLCs, large differences in electrochemical properties become apparent when the same electrodes are combined with different types of electrolytes. Therefore, it was crucial to test the electrochemical properties of the obtained GO/CNTs electrode with different types of electrolytes.

More and more battery companies and scientists are putting effort into solid-state energy storage devices research during the past few years. Solid-state batteries have advantages in safety, efficiency, working environment, lifetime, etc. It is a good start to investigate all-solid-state supercapacitors since they have a very similar structure when comparing with batteries.

#### 4.2 Experimental Design

##### 4.2.1 Equipment and Personal Safety Equipment

Equipment:

- Stainless steel tweezer
- Paper knife
- Scale and weigh paper
- Stainless steel ruler

Safety equipment:

- Long sleeved lab coat
- Safety goggles
- Anti-corrosion plastic gloves

#### 4.2.2 Sulfuric Acid ( $H_2SO_4$ )

Sulfuric acid has high conductivity and low internal resistance, which makes it one of the most commonly used liquid electrolytes. Ions easily penetrate the micropores of the electrode because of their small molecular diameter. Additionally, compared with that of organic electrolytes, sulfuric acid has advantages in longevity, conductivity, thermal capacity, and environmental impact. Sulfuric acid is cheap and has no special requirements during the assembly process making it the perfect electrolyte candidate in the lab.

In this experiment, a simple three-layer sandwich-structured EDLC was made with obtained binder-free electrodes with 1 M sulfuric acid solution. The sulfuric acid was filled in between the two GO/CNTs layers and separated by a porous polypropylene separator (Celgard 3401). Two copper films (1 cm width) were used to extend both the positive and negative substrates for an easier connection with wires. Two clips were applied on the device to ensure a moderate pressure between the two electrodes; the pressure provided the electrodes and electrolyte a better contact. Some samples are shown below.



Figure 7: The top two samples were GO/CNTs with an  $H_2SO_4$  electrolyte; the bottom two samples were GO/CNTs with a PVA/ $H_3PO_4$  gel electrolyte.

Two sets of samples were made during the experiment, with one set using the obtained binder-free electrodes with 1M sulfuric acid. The other set used the GO/CNTs film as electrodes with gel electrolyte. Both sets were made into a symmetrical structure.

For this, it must be noted that all aqueous electrolytes also had shortcomings. The major issue was that the devices will have a narrow electrochemical window by using an aqueous electrolyte due to the positive electrode having an oxygen evolution reaction when the potential reached 1.23 V [23].

## 4.2.3 Gel Electrolyte

### 4.2.3.1 Introduction

Poly(vinyl alcohol) (PVA)-based aqueous gel electrolytes, such as PVA/H<sub>2</sub>SO<sub>4</sub>, PVA/KOH and PVA/LiCl, are widely used to transfer ions between two electrodes in sandwich-typed solid-state supercapacitors. Therefore, it has great potential to combine with the obtained binder-free electrodes to achieve better electrochemical performance.

Similar to the setup in the previous section, symmetrical sandwich-structured EDLCs were assembled except that the aqueous electrolyte was substituted for the gel electrolyte material. From different angles, the solid-state electrolyte is a perfect candidate for energy storage devices in the future. These environmentally friendly electrolytes have great conductivity, stable properties, a small grain boundary resistance, a matched thermal expansion coefficient with electrodes, a high working voltage, and a wide working temperature range. Therefore, there are far-reaching advantages if existing energy storage devices are promoted to an all-solid-state level, which has high electrochemical performance.

Due to an easier fabrication process and appropriate chemical properties, PVA-based material was the most suitable candidate for fabricating gel electrolytes at this stage. Two types of PVA-based gel electrolytes (PVA/H<sub>2</sub>SO<sub>4</sub> gel and PVA/H<sub>3</sub>PO<sub>4</sub> gel) were investigated and tested in this study. By applying PVA-based gel electrolyte into the obtained GO/CNTs binder-free electrodes, an all-solid-state EDLC was achieved. The GO/CNTs electrode in a square shape had a length of 5 cm; the square-shaped gel electrolyte had a length of 5.5 cm to ensure that the two electrodes were separated

completely. The PVA/H<sub>2</sub>SO<sub>4</sub> gel electrolyte had a thickness of 1.5 mm, and the thickness of the PVA/H<sub>3</sub>PO<sub>4</sub> gel was 0.5 mm. After assembly of the PVA-based gel electrolyte with the obtained binder-less electrodes, a comparison with the devices using aqueous electrolytes was performed, as described in the next chapter. The PVA-based gel electrolyte showed great potential for moving forward with all-solid-state EDLCs if we add MnO<sub>2</sub> or an ion source to make hybrid capacitors in the future.

The typical specific capacitance for a PVA based gel electrolyte EDLC is usually between 11.8 F/g and 136 F/g [24]. This is even higher than some aqueous, organic or ionic liquid electrolyte supercapacitor. PVA based electrolytes provided a wide potential window of 0-1.6 V. For other polymer-based solid electrolytes (for example PMMA based), it reached 0-4.8 V with a 0.174 Wh/g energy density [25]. Therefore, the solid polymer electrolyte had a great potential to make a safer, cheaper, a more environmentally friendly supercapacitor with a wide potential window and a high energy density at the same time.

#### **4.2.3.2 PVA with H<sub>2</sub>SO<sub>4</sub>**

According to Narendra and his team's work [26], 1 gram of H<sub>2</sub>SO<sub>4</sub> was added into 10 milliliters of deionized water. Then, 1 gram of PVA powder was added to the solution. The whole mixture was heated to 85 degrees Celsius while stirring until the solution became clear. Finally, the entire mixture was solidified at room temperature for one hour or longer. The above procedure was also followed in this particular experiment to obtain the same results. The obtained PVA/H<sub>2</sub>SO<sub>4</sub> gel electrolyte is shown below. Two three-layer sandwich samples were made and tested in the next chapter. However, due to their

corrosive nature and mediocre performance, the PVA/H<sub>2</sub>SO<sub>4</sub> gel electrolyte was not selected as the first gel electrolyte candidate for this study.

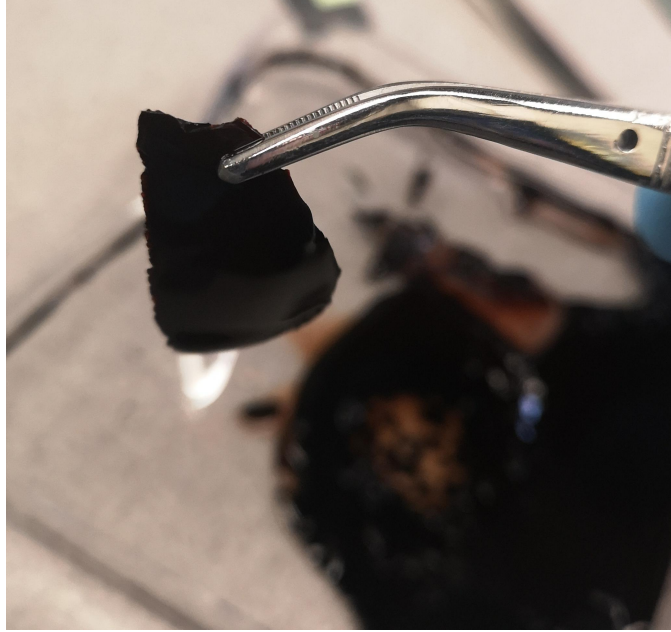


Figure 8: A picture of the PVA/H<sub>2</sub>SO<sub>4</sub> gel electrolyte piece.

#### 4.2.3.3 PVA with H<sub>3</sub>PO<sub>4</sub>

Based on Mengyao and her team's work [27], an modified method for making a PVA/H<sub>3</sub>PO<sub>4</sub> gel electrolyte was achieved here.

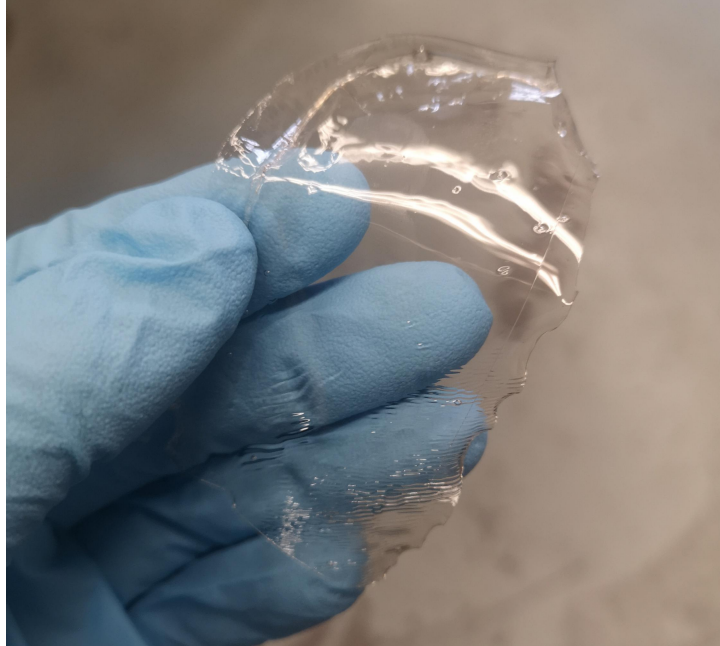


Figure 9: A picture of the PVA/H<sub>3</sub>PO<sub>4</sub> gel electrolyte piece.

In this simplified method, first, 6 grams of PVA powder and 6 grams of H<sub>3</sub>PO<sub>4</sub> were dissolved in 60 milliliters of deionized water. Then, the mixture was stirred at 85 degrees Celsius until the solution changed to a transparent liquid state with high viscosity. Finally, the mixture was poured into a shallow glass container and heated in an oven for 30 minutes at 85 degrees Celsius. Once it solidified into a gel, it was placed under a fume hood and dried to room temperature.

The PVA/H<sub>3</sub>PO<sub>4</sub> gel electrolyte was combined with the binder-free electrode to make a sandwich-structured EDLC. To make a better comparison, an additional set of PVA/H<sub>3</sub>PO<sub>4</sub> gel electrolytes was tested with commercial supercapacitor electrodes (film electrodes disassembled from a Maxwell BCAP3000). The existing commercial electrodes were separated and extracted from a Maxwell supercapacitor (2.7 V, 3000 Farad). The test results are presented in Chapter 5.



## CHAPTER 5

### TESTING AND RESULTS

#### 5.1 Method and Equipment

Several methods were used for conducting this experiment. These methods required various equipment to ensure the development of binder-free EDLCs.

##### 5.1.1 Cyclic Voltammetry (CV)

Cyclic voltammetry (CV) is one of the most expedient techniques to measure the current status under different potential conditions. By using an electrochemical analyzer from CH Instruments (Model CHI 660 E), a voltammogram (current VS. potential graph) was obtained and used to analyze the voltage window as well as the capacitance. It is worth noting that due to the sweep of the applied potential, the tested sample is charged and discharged multiple times. Therefore, the sample is aged with an increasing number of test cycles, but on the other hand, this feature can be used to calculate the lifetime of the sample. Cycle life testing is a time-consuming process and since it was not the priority objective of this study, that testing was skipped for the time being.

According to Ohm's Law for capacitors, the capacitance  $C$  is related to the current  $I$  through the capacitor and changing rate of voltage  $V$ , which can be expressed by:

$$I = C * \frac{dV}{dt}$$

Cyclic voltammetry was plotted with the current on the y-axis and voltage on the x-axis. Under a certain scan rate, each charging and discharging cycle was formed into a rectangular shape in a CV plot for an ideal capacitor. In the actual testing, two corners of the rectangle were rounded due to the ESR of the device. Each closed rectangular cycle contained both the charging and discharging process, which meant the closed area of a CV cycle was twice high as the actual power of the device. The power  $P$  of a capacitor can be calculated using the basic electrical power equation:

$$P = I * V$$

Thus, once the area of a cycle from CV was calculated, the power of the device was half of it. Then, the power of the capacitor was divided by its scan rate. This was followed by dividing by its potential range, which calculated the capacitance under the scan rate of this device written below:

$$C = \left(\frac{P}{dV/dt}\right)/V$$

This can also be written in an alternate form:

$$C = \frac{I}{dV/dt}$$

## 5.1.2 Electrochemical Impedance Spectroscopy (EIS)

### 5.1.2.1 Introduction

Electrochemical impedance spectroscopy (EIS) is a widely used technique to observe the associated impedance response of energy storage devices, which refers to the frequency-dependent resistance to an alternating current (AC) flow of a circuit element [28]. In this study, EDLCs were used. As a supercapacitor can be modeled as a network of passive electrical circuit elements, the response from EIS of this equivalent circuit was calculated and treated as the actual EIS response of the supercapacitor. Due to its testing mechanism, the tested samples were not aging or decaying under EIS investigation. The major work was performed by a Gamry's potentiostatic EIS (Model reference 600), and the plot was drawn by Gamry's Sequence Wizard analyzing software.

The Bode plot from the EIS analysis was a graph of the frequency response of the system, which expressed the phase shift of the supercapacitor under different frequencies ( $\omega$ ). The impedance ( $Z_\omega$ ) was plotted with the log of frequency on the x-axis and both the absolute value of the impedance ( $|Z| = Z_0$ ) and the phase-shift on the y-axis [29].

$$Z_\omega = \frac{E_\omega}{I_\omega}$$

In this case,  $E_\omega$  was the frequency-dependent potential, and  $I_\omega$  was the frequency-dependent current.

EIS data can also be presented as a Nyquist (complex plane) plot. A typical Nyquist plot for supercapacitors was made of two shapes: a semicircle and a linear straight line. The system was kinetically facile if the semicircle region was small;

however, if the system was kinetically slow, the straight line dominated more of the region, and the mass transfer was more significant in the system.

The open circuit potential of each sample was also measured through potentiostatic EIS. The plot showed how the voltage changed in an open circuit system over time.

### 5.1.2.2 Randles Model

To analyze the tested results from EIS, the simplest Randles circuit model was applied to describe the investigated system [see schematic below]. The model consisted of a resistance  $R_e$ , which was the sum of resistances from the electrodes, electrolyte, and electrical contacts. The equivalent series resistance  $R_e$  was in series with the parallel combination of an ideal double-layer capacitance  $C$  and a small leakage resistance  $R_i$ , which was the impedance from a faradaic reaction. Impedance spectra were more complicated in a real EDLC system, but the Randles equivalent circuit provided the simplest possible models to describe processes at the electrochemical interface [29].

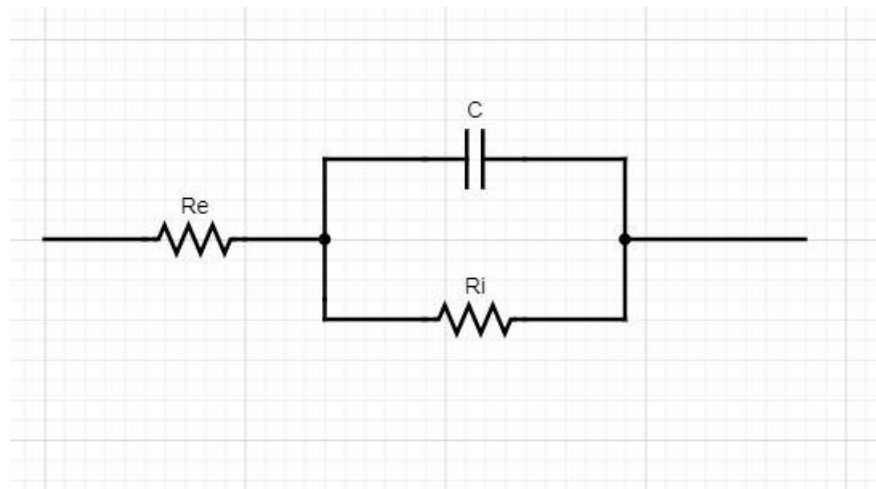


Figure 10: Schematic of the simplest and most common Randles circuit.

## 5.2 Results and Analysis

### 5.2.1 Obtained GO/CNTs electrodes with the H<sub>2</sub>SO<sub>4</sub> electrolyte

As mentioned in Chapter 4, H<sub>2</sub>SO<sub>4</sub> is the most commonly used electrolyte due to its ease of use. In this section, the obtained GO/CNTs binder-free electrodes were combined with sulfuric acid at first. The EIS showed that a 5 cm by 5 cm sample performed their best specific capacitance value of 0.02788 F/m<sup>2</sup> in volumetric terms and 5.646 mF/g in gravimetric terms. The lowest ESR for the sample was only 0.07 Ohms (70 mΩ), which was very impressive when compared with those of existing supercapacitors (3 Ohms from Chen's work, which was a carbon nanotube array electrode with 1 M sulfuric acid used as electrolyte) [30].

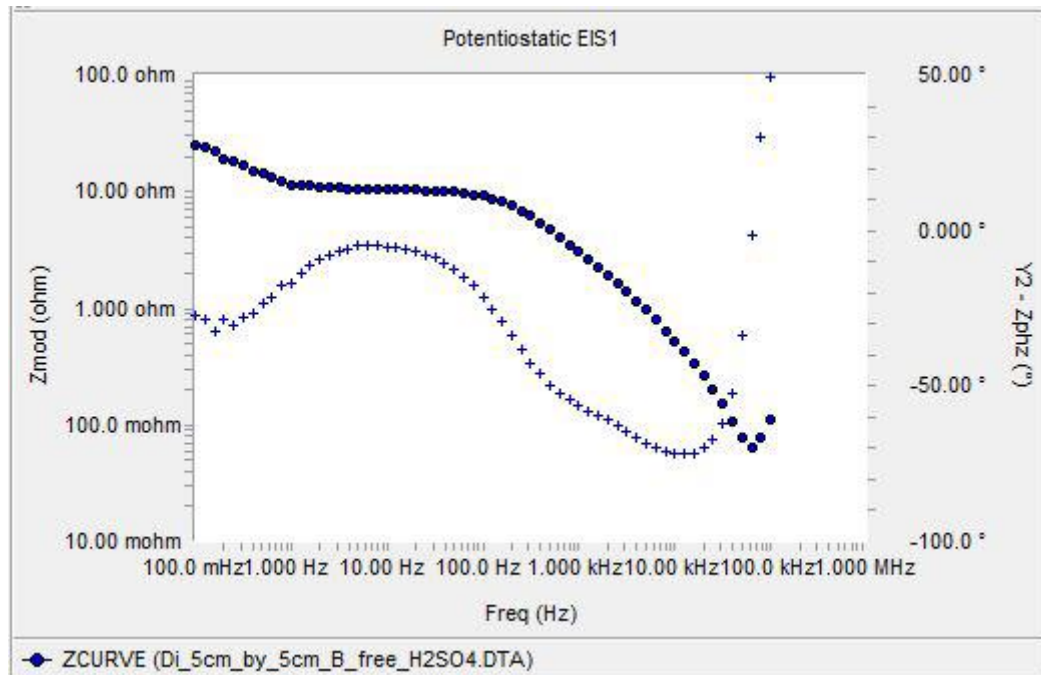


Figure 11: Bode diagram of the obtained GO/CNTs electrode with H<sub>2</sub>SO<sub>4</sub> electrolyte.

The EIS magnitude is shown as the dotted line, and the phase is shown as the cross line. Above 100 kHz, the bulk of the ESR domain is in this region. In the region between 1 Hz and 100 Hz, the capacitance primarily controls the impedance.

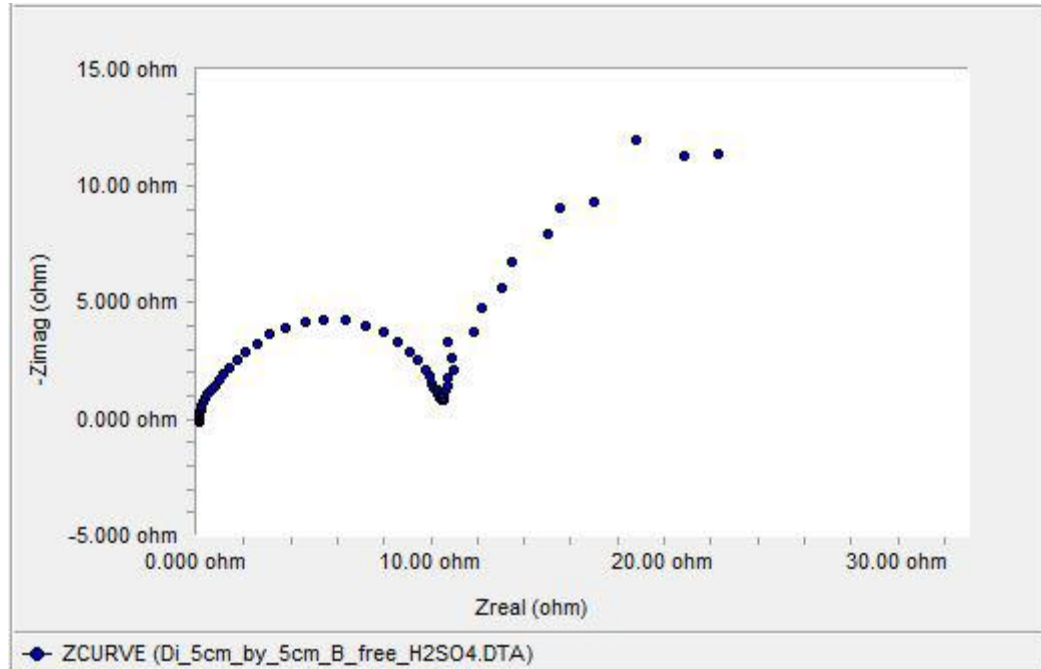


Figure 12: Nyquist diagram of the obtained GO/CNTs electrodes with the H<sub>2</sub>SO<sub>4</sub> electrolyte.

In a Nyquist plot, the starting value on the far left is attributed to the internal resistance which is the sum of the resistance of the bulk electrolyte, the electrode, and the contact resistance between the electrode and the current collector. The critical point on the right of the semicircle can be treated as the charge transfer resistance. The existence of the nonvertical line on the right side was attributed to the equivalent distribution resistance.

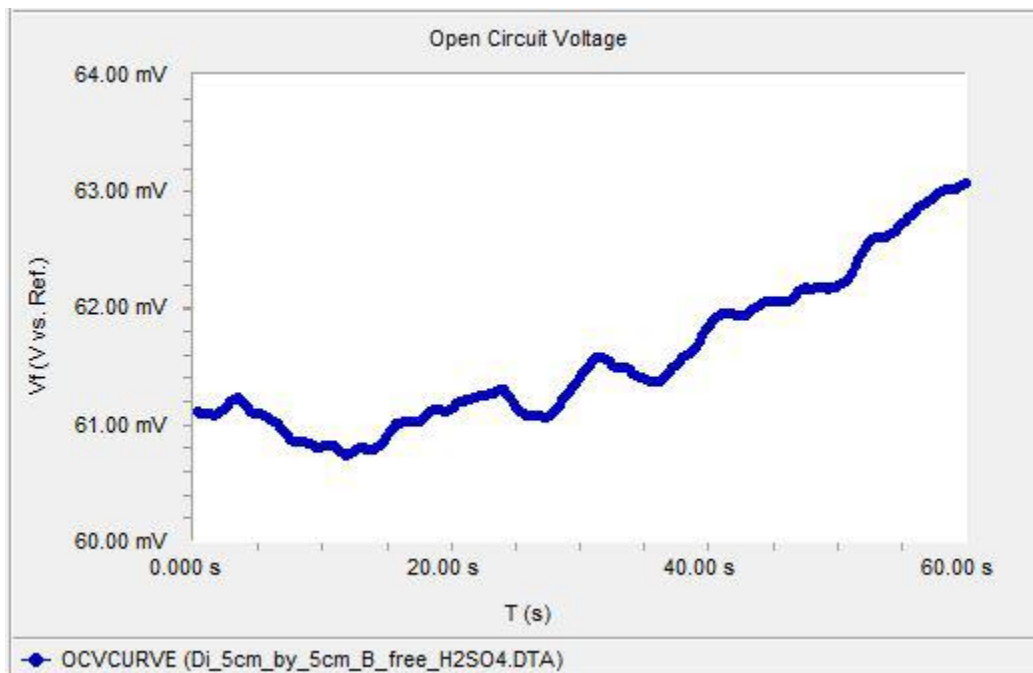


Figure 13: Open circuit voltage diagram of the obtained GO/CNTs electrodes with the H<sub>2</sub>SO<sub>4</sub> electrolyte.

### 5.2.2 Obtained GO/CNTs electrodes with the PVA/H<sub>3</sub>PO<sub>4</sub> gel electrolyte

By using the PVA/H<sub>3</sub>PO<sub>4</sub> gel electrolyte instead of sulfuric acid, the device performed at a specific capacitance of 1.406 F/m<sup>2</sup>. The results were competitive with the results of other all-solid-state EDLC devices.

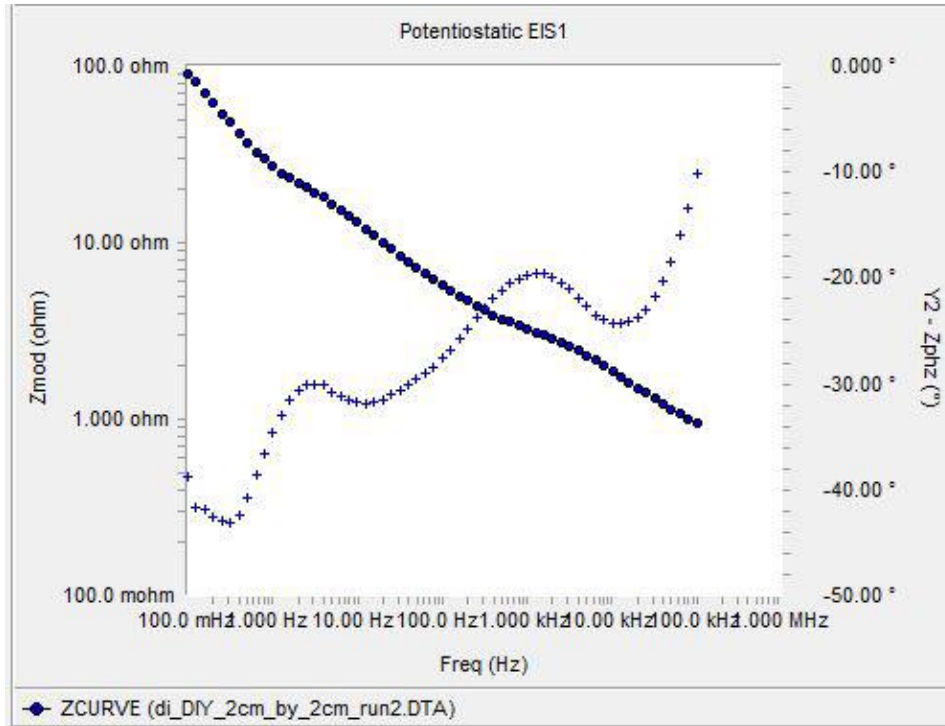


Figure 14: Bode diagram of the obtained GO/CNTs electrodes with the PVA/ H<sub>3</sub>PO<sub>4</sub> gel electrolyte.

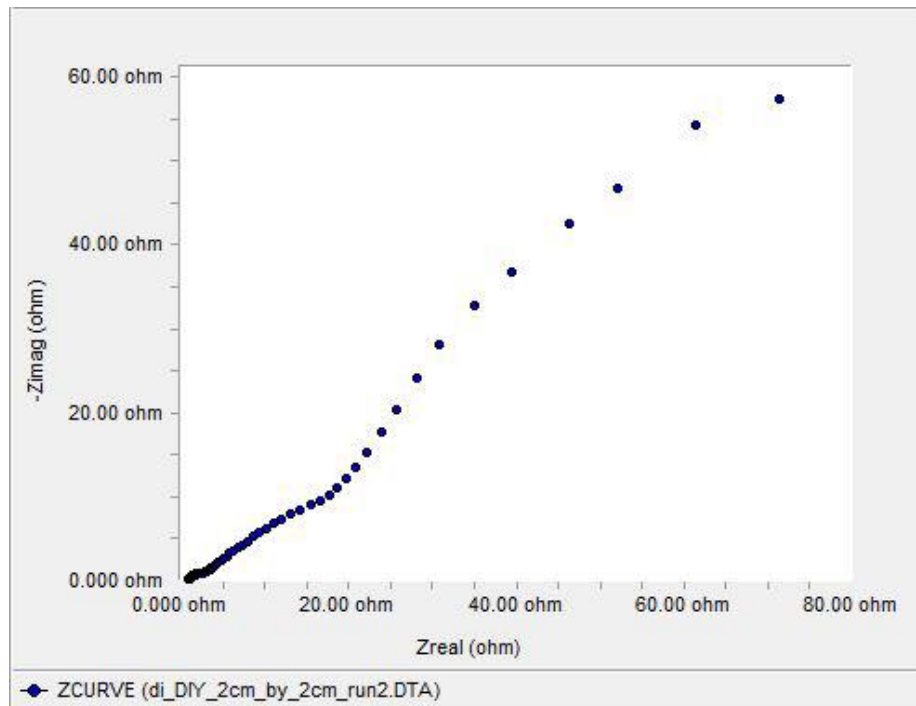


Figure 15: Nyquist diagram of the obtained GO/CNTs electrodes with the PVA/H<sub>3</sub>PO<sub>4</sub> gel electrolyte.



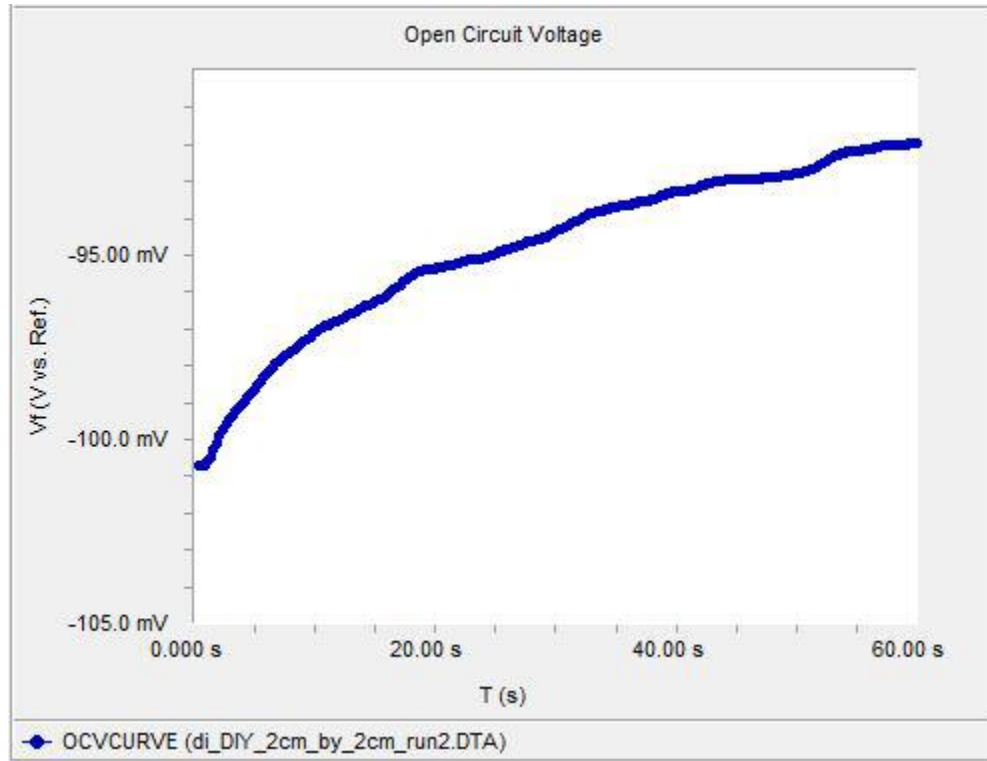


Figure 16: Open circuit voltage diagram of the obtained GO/CNTs electrodes with the PVA/ H<sub>3</sub>PO<sub>4</sub> gel electrolyte.

### 5.2.3 Obtained GO/CNTs electrodes with the PVA/H<sub>2</sub>SO<sub>4</sub> gel electrolyte

With the use of a PVA/H<sub>2</sub>SO<sub>4</sub> gel electrode and the obtained GO/CNTs binder-free electrodes, the sample performed at a specific capacitance of 0.04436 F/m<sup>2</sup> with a low ESR of 2.305 Ohms. The higher value of ESR and lower capacitance made the PVA/H<sub>2</sub>SO<sub>4</sub> gel electrolyte superior when compared with those of the PVA/H<sub>3</sub>PO<sub>4</sub> gel electrolyte in the previous section.

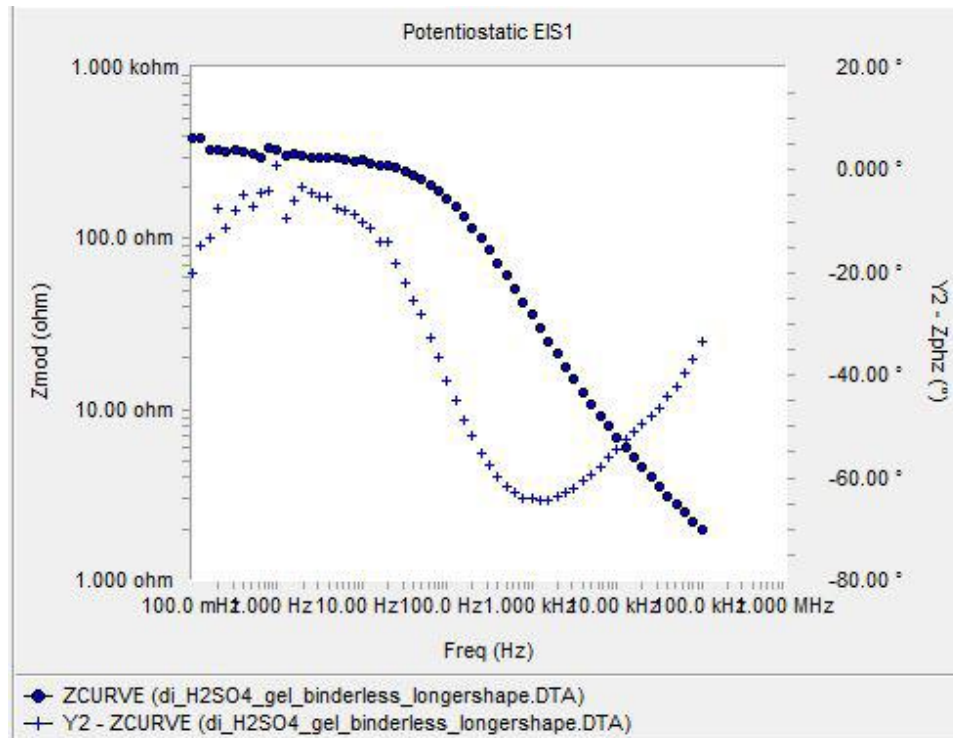


Figure 17: Bode diagram of the obtained GO/CNTs electrodes with the PVA/ H<sub>2</sub>SO<sub>4</sub> gel electrolyte.

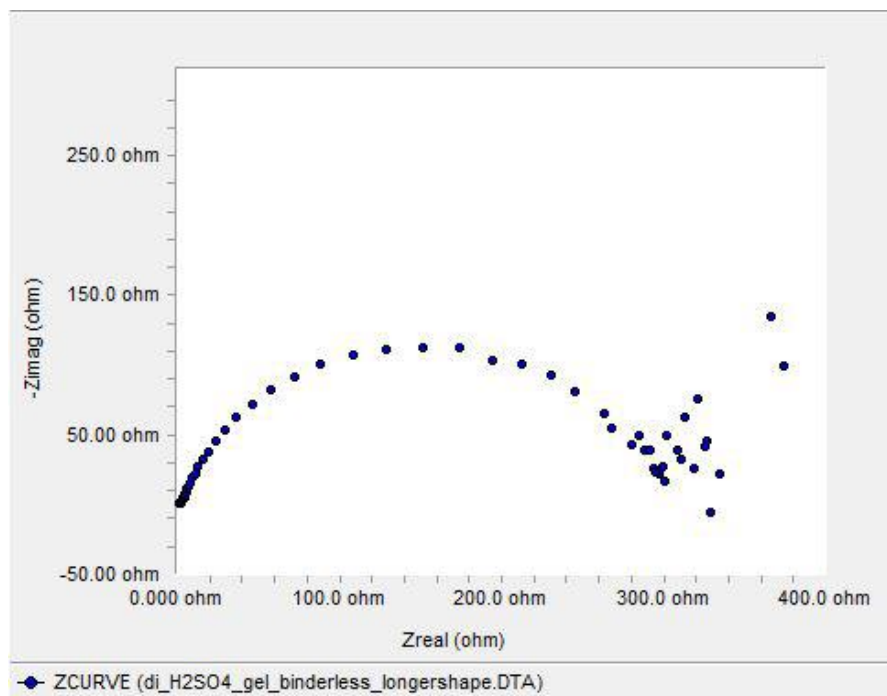


Figure 18: Nyquist diagram of the obtained GO/CNTs electrodes with the PVA/ H<sub>2</sub>SO<sub>4</sub> gel electrolyte.

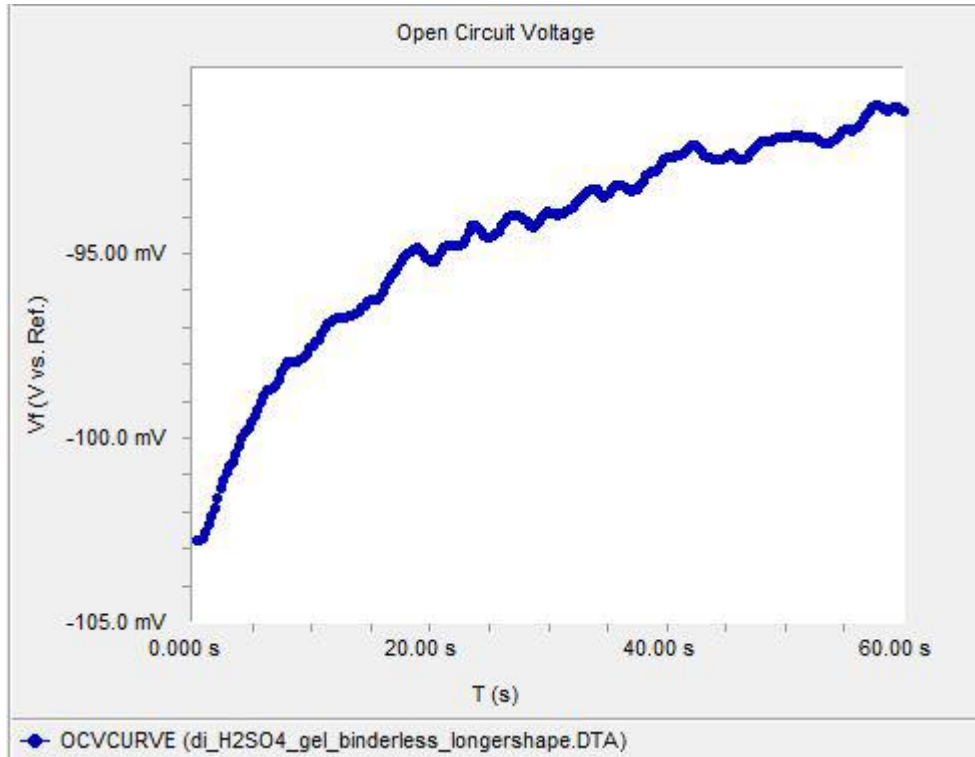


Figure 19: Open circuit voltage diagram of the obtained GO/CNTs electrodes with the PVA/ H<sub>2</sub>SO<sub>4</sub> gel electrolyte.

#### 5.2.4 Maxwell electrode with the PVA/H<sub>3</sub>PO<sub>4</sub> gel electrolyte

Through an EIS investigation, the best results were obtained by combining commercial electrode films (from Maxwell) with the PVA/H<sub>3</sub>PO<sub>4</sub> gel electrolyte; the above-prepared EDLC had a specific capacitance of 4.841 F/m<sup>2</sup> with a resistance of 178 Ohms.

The high resistance was probably caused by the double-sided coating of the electrode film, which provided extra resistance to the device. The mature manufacturing process and its thick electrode coating on the substrate greatly impacted the great performance in capacitance. Due to the value of ESR from the Maxwell electrode, which

was approximately 100 times higher than the obtained GO/CNTs electrode, we can say that the binder-free electrode from this study had successfully decreased the resistance. In addition, testing based on different variables still needed to investigate the resistance reduction between Maxwell electrode and obtained binder-free electrode. More details are discussed in Chapter 7.

has a better electrochemical performance.

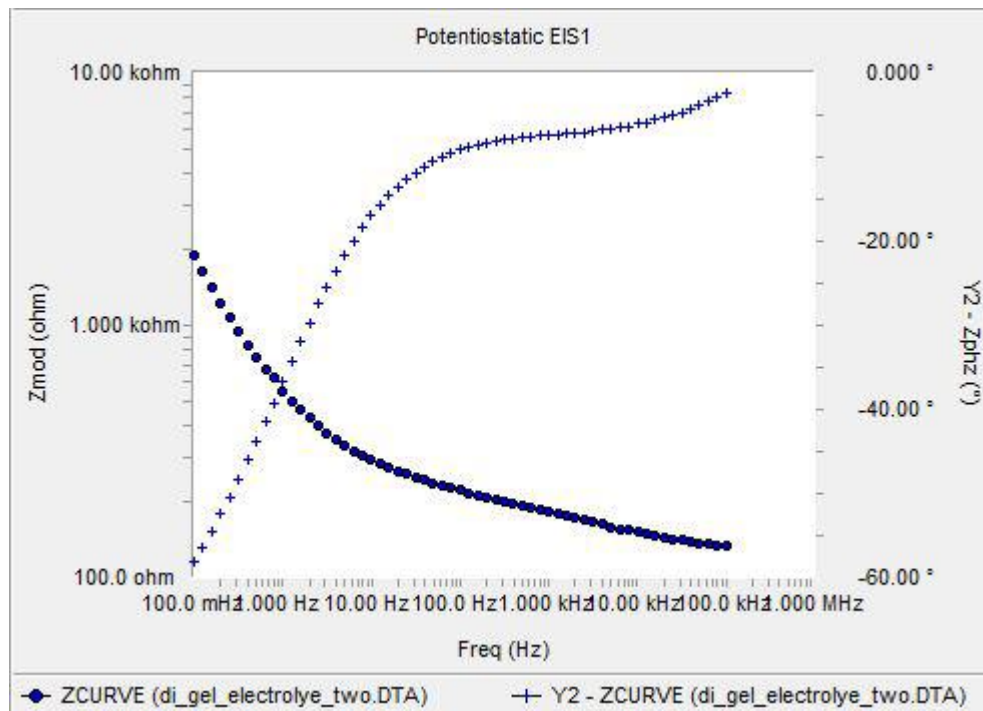


Figure 20: Bode diagram of the Maxwell electrode with the PVA/H<sub>3</sub>PO<sub>4</sub> gel electrolyte.

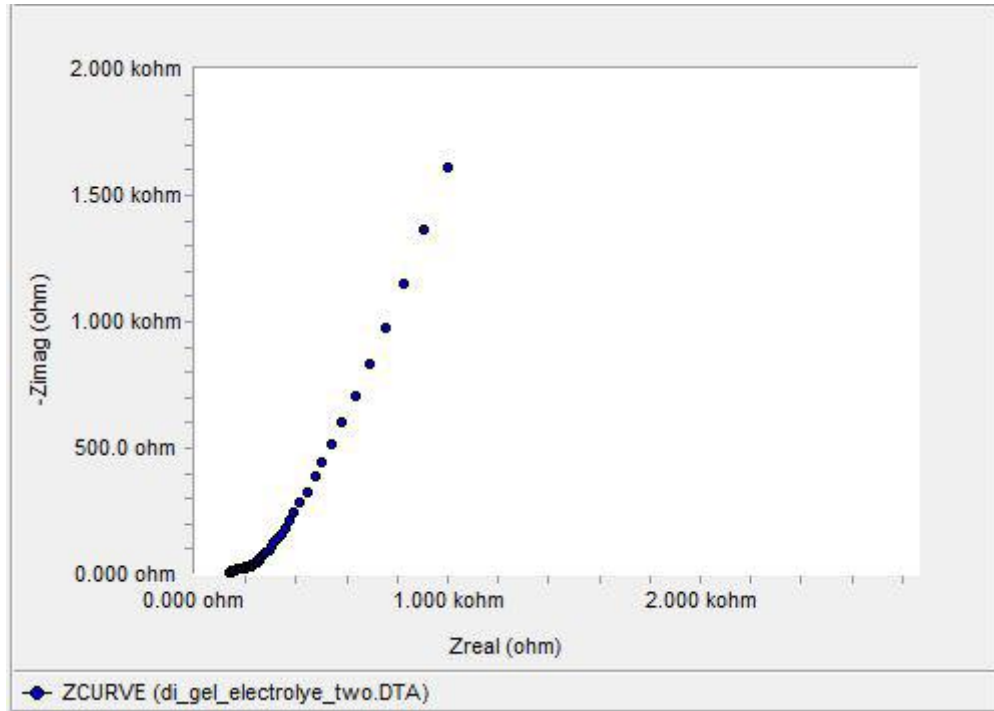


Figure 21: Nyquist diagram of the Maxwell electrode with the PVA/H<sub>3</sub>PO<sub>4</sub> gel electrolyte.

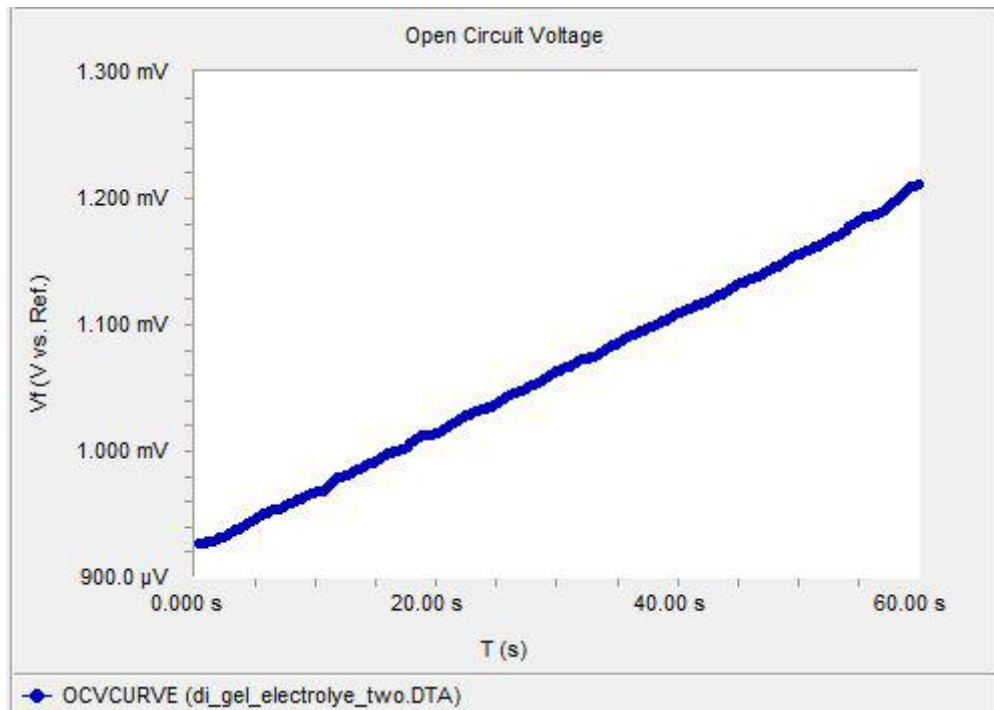


Figure 22: Open circuit voltage diagram of the Maxwell electrode with the PVA/H<sub>3</sub>PO<sub>4</sub> gel electrolyte.

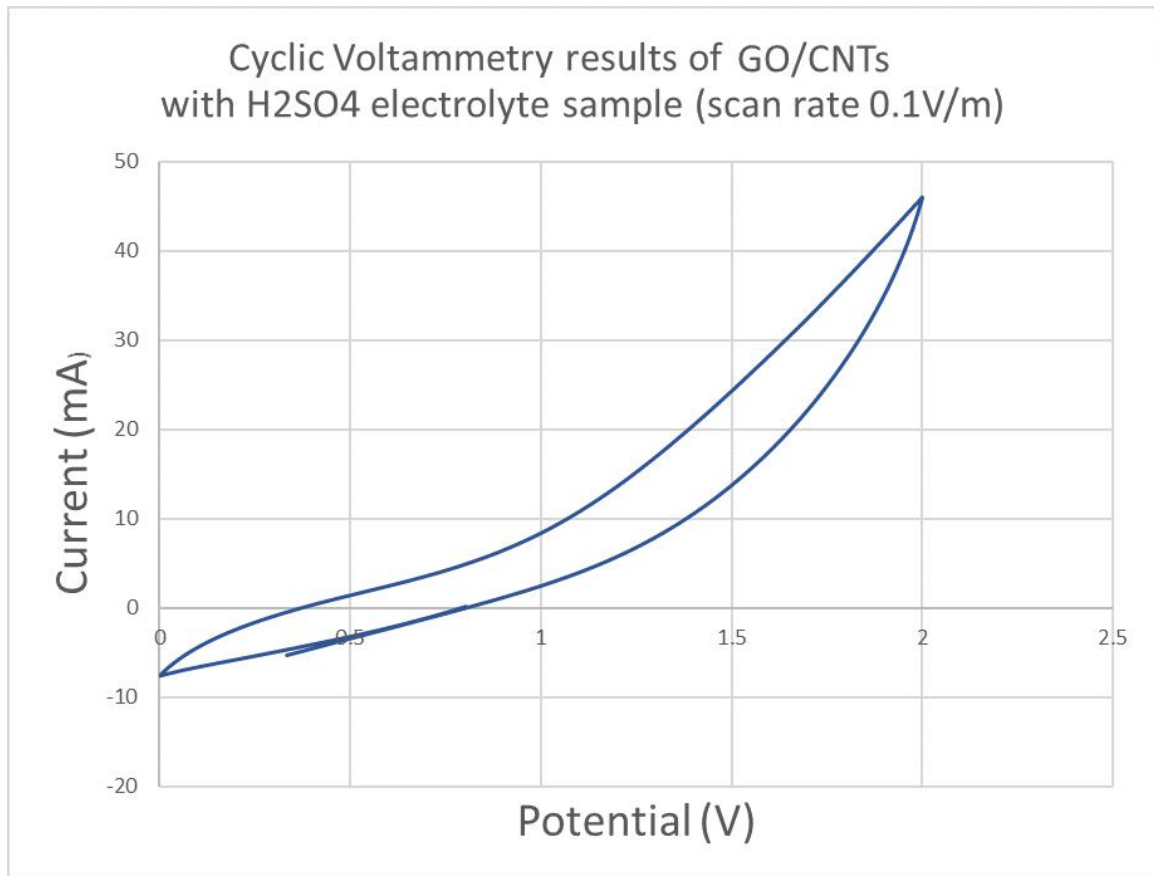


Figure 23: Cyclic voltammetry diagram of GO/CNTs electrode with the H<sub>2</sub>SO<sub>4</sub> electrolyte. The sample was tested from 0 V to 2 V under a 0.1 V/s scan rate.

From the cyclic voltammetry plot, the enclosed area of the cycle was calculated by using OriginLab software. The capacitance of the sample under a 0.1 V/s scan rate was calculated to have a value of 0.03157 Farads (31.57 mF).

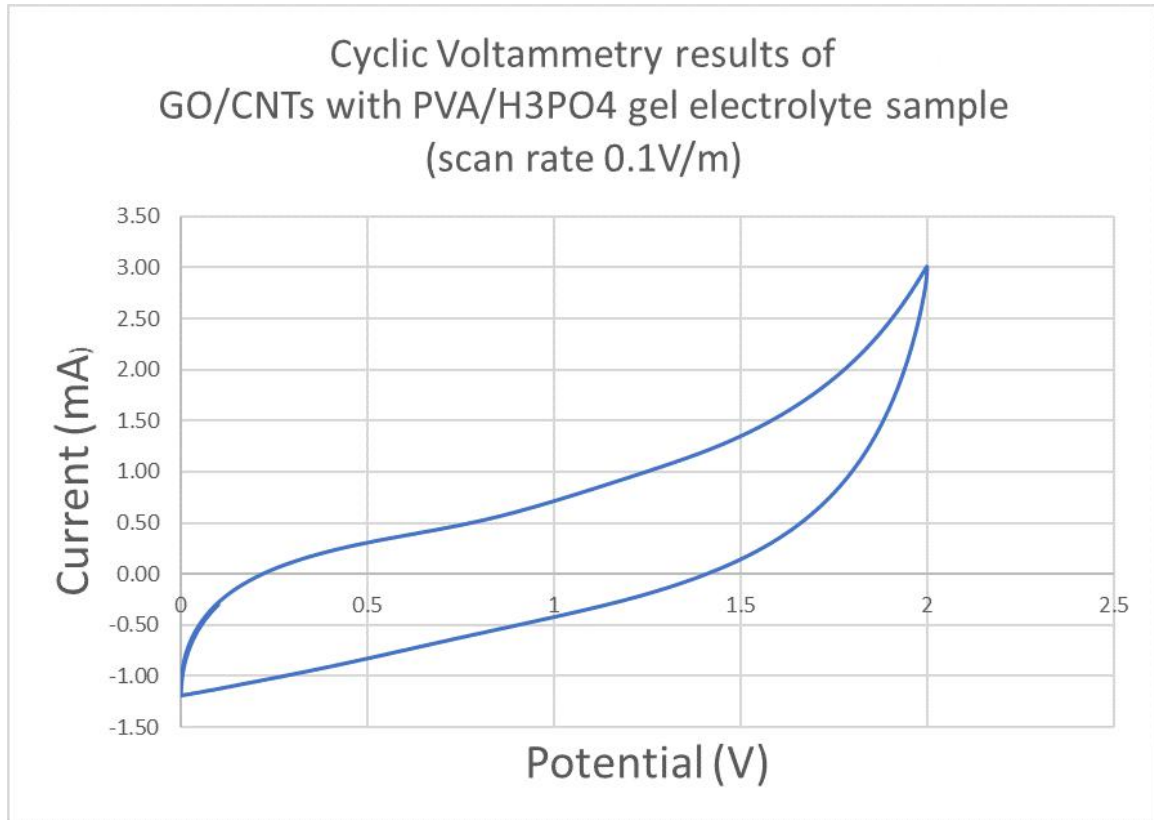


Figure 24: Cyclic voltammetry diagram of GO/CNTs electrode with the PVA/H<sub>3</sub>PO<sub>4</sub> gel electrolyte. The sample was tested from 0 V to 2 V under a 0.1 V/s scan rate.

From the cyclic voltammetry plot, the enclosed area of the cycle was calculated by using OriginLab software. The capacitance of the sample under a 0.1 V/s scan rate was calculated to have a value of 0.005417 Farads (5.417 mF).

## CHAPTER 6

### CONCLUSION

Different sets of results were achieved during this study. Based on all the experimental results from Chapter 5, as seen in Table 1, by using the same electrode, a PVA/H<sub>3</sub>PO<sub>4</sub> gel-based solid-state EDLC obtained a specific capacitance that was 73 times higher than that of an aqueous-based EDLC. Overall, the lowest ESR from the obtained GO/CNTs binder-free electrode had a better than average value of 0.07 Ohms, which was very impressive.

In the GO/CNTs binder-free electrode sample, 1 M sulfuric acid was used as the electrolyte, and a porous polypropylene separator was placed between the two electrodes.

Chapter Number	Electrode Material	Electrolyte Material	Specific Capacitance (F/m <sup>2</sup> )	Specific Capacitance (mF/g)	ESR (Ω)
5.2.1	GO/CNTs ①	H <sub>2</sub> SO <sub>4</sub>	0.01938	2.4225	0.07
5.2.1	GO/CNTs ②	H <sub>2</sub> SO <sub>4</sub>	0.02788	5.646	0.4241
5.2.2	GO/CNTs	PVA/H <sub>3</sub> PO <sub>4</sub>	1.406	-	1.554
5.2.3	GO/CNTs	PVA/H <sub>2</sub> SO <sub>4</sub>	0.04436	-	2.305
5.2.4	Maxwell	PVA/H <sub>3</sub> PO <sub>4</sub>	4.841	-	178

Table 1: EIS results of all samples.

① is the trial with lowest ESR, ② is the trial with the highest specific capacitance)



Compared with that of the existing studies of EDLCs, SaiSai [31] and his team showed a result with a specific capacitance of  $0.2 \text{ F/m}^2$  by using graphitic carbon spheres as electrodes and KOH as an electrolyte, which was lower than the all-solid-state binder-free EDLC from this study. Young and his team [32] studied reducing the ESR for EDLCs. The work showed that by using chemical vapor deposition-grown graphene (CVD-G) as an electrode, a low ESR of 0.23 Ohms was obtained in an aqueous electrolyte, which was 3.3 times higher than the 0.07 Ohms from the binder-free electrode with aqueous electrolyte in this study.

Due to a rough and limited processing and other objective factors, all samples fabricated during this study still have much room for quality improvement. For example, using a better technique to obtain a much more evenly distributed electrode coating; using a customized heating system instead of the hot plate to evaporate the water content of slurry more smoothly and assembling all of the parts in a glove box to remove contamination, are just a few possible improvements.

Overall, a binder-free electrode was achieved during this study. The obtained electrodes had a very low ESR when using an aqueous electrolyte. By combining with a PVA-based gel electrolyte, a solid-state EDLC with great performance was acquired.

## CHAPTER 7

### FUTURE WORK

#### 7.1 Laser Treatment

The energy capacity of EDLCs directly depends on its specific surface area. So, laser treatment can be applied to further increase the surface area. According to Mingmao and his team's results [33], laser-carved reduced graphene oxide (rGO) film readily produces rGO interdigital micropatterns. Those micropatterns provided extra cavities for storing ions. So, the use of laser exfoliation is worth to explore to increase the specific energy in the future.

#### 7.2 Electrode Fabrication

A mass production solution of GO/CNTs film is a promising start for developing an easier fabrication method of binder-free electrodes. Furthermore, this can be done by a roll-to-roll technique. Then, the fabricated electrode film can be rolled up with gel electrolyte films to manufacture cylinder-type supercapacitors.

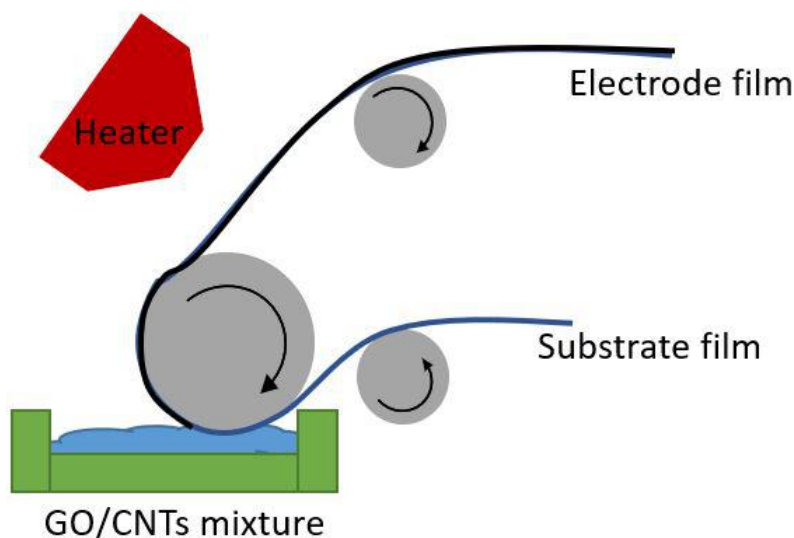


Figure 25: Illustrator of a roll-2-roll production line.

The aluminum substrate goes into a slurry tank by a driving roller, The casted side with electrode slurry then dried by heating source and the finished film can be used as electrode directly.

### 7.3 Electrolyte Fabrication

During the fabrication process of the PVA/H<sub>3</sub>PO<sub>4</sub> gel electrolyte, a solution is obtained by mixing H<sub>3</sub>PO<sub>4</sub> and PVA, and a gel film can easily be attained by heating the mixture. Therefore, a heating roller in the roll-to-roll system can be suggested. The gel electrolyte film can then also be mass-produced. Furthermore, an electrolyte fabricating system can also be assembled with the electrode production line mentioned in the previous section.

## 7.4 Hybrid Capacitor

The electrochemical performance of the EDLC was limited by its symmetric structure. In actual applications, ion sources are usually added, for example, lithium hydroxide (LiOH), into an electrolyte to improve its power density. Or they might add an oxidizing agent, for example, manganese dioxide (MnO<sub>2</sub>), into one electrode to improve its energy density. It may be possible to upgrade an obtained binder-free all-solid-state EDLC to a hybrid capacitor to compete with existing energy storage devices. All of the results in this study help in understanding the importance of these energy storage devices and the several steps that can be taken for the improvement of these devices.

## BIBLIOGRAPHY

- [1]. M.F. El-Kady, R.B. Kaner, Nat. Commun. 4 (2013) 1475-1484.
- [2]. Y. Gogotsi, Nature 509 (2014) 568-570.
- [3]. X. Feng, N. Chen, J. Zhou, Y. Li. Z. Huang, L. Zhang, Y. Ma, L. Wang, X. Yan, New J. chen. 39 (2015) 2261-2268.
- [4]. H. Cheng, Z. Dong, C. Hu, Y. Zhao, Y. Hu, L. Qu, N. Chena, L. Dai, Nanoscale 5 (2013) 3428-3434.
- [5]. S. Chen, W. Ma, Y. Cheng, Z. Weng, B. Sun, L. Wang, W. Cheng, F. Li, M. Zhu, H. M. Cheng, Nano Energy 15 (2015) 642-653.
- [6]. W. Ma, S. Chen, S. Yang, W. Chen, Y. Cheng, Y. Guo, S. Peng, S. Ramakrishna, M. Zhu, J. Power Sources 306 (2016) 481-488.
- [7]. Science. July 5, 2019, Vol. 365 Issue 6448, p37, 1 p.
- [8]. Xian J.; Shiyu L; "Carbon-Based Electrode Materials for Supercapacitor: Progress, Challenges and Prospective Solutions" Journal of Electrical Engineering 4(2016)75-87.
- [9]. Patrice Simon; Andrew Burke. Spring 2008. "Nanostructured Carbons: Double-Layer Capacitance and More" The Electrochemical Society.
- [10]. Chem. Soc. Rev., 2015, 44, 7484-7539.

- [11]. Zhao, Cuimei, and Weitao Zheng. "A Review for Aqueous Electrochemical Supercapacitors." *Frontiers*, Frontiers, 24 Apr. 2015, [www.frontiersin.org/articles/10.3389/fenrg.2015.00023/full](http://www.frontiersin.org/articles/10.3389/fenrg.2015.00023/full).
- [12]. Abruña, H. D.; Kiya, Y.; Henderson, J. C. (2008). "*Batteries and Electrochemical Capacitors*" (PDF). *Phys. Today*. 61 (12): 43–47.
- [13]. Béguin, Francois; Raymundo-Piñero, E.; Frackowiak, Elzbieta (2009). "8. *Electrical Double-Layer Capacitors and Pseudocapacitors*". *Carbons for Electrochemical Energy Storage and Conversion Systems*. CRC Press. pp. 329–375. doi:10.1201/9781420055405-c8. ISBN 978-1-4200-5540-5.
- [14]. Texas Instruments, Characteristics of Rechargeable Batteries, SNVA533.
- [15]. Xiong, Guoping & Kundu, Arpan & S. Fisher, Timothy. (2015). Influence of Temperature on Supercapacitor Performance. 10.1007/978-3-319-20242-6\_4.
- [16]. *J. Mater. Chem.*, 2012, 22, 3591.
- [17]. "*Binderless Electrodes for High-Temperature Polymer Electrolyte Membrane Fuel Cells*." *Journal of Power Sources*, Elsevier, 4 Sept. 2014.
- [18]. X. J. Lu, H. Dou, B. Gao, C. Z. Yuan, S. D. Yang, L. Hao, L. F. Shen and X. G. Zhang, *Electrochim. Acta*, 2011, 56, 5115–5121.
- [19]. D. S. Yu and L. M. Dai, *J. Phys. Chem. Lett.*, 2010, 1, 467–470.
- [20]. L. Qiu, X. W. Yang, X. L. Gou, W. R. Yang, Z. F. Ma, G. G. Wallace and D. Li, *Chem.–Eur. J.*, 2010, 16, 10653–10658.
- [21]. H. R. Byon, S. W. Lee, S. Chen, P. T. Hammond and Y. Shao-Horn, *Carbon*, 2011, 49, 457-467.

- [22]. Stokes, Debbie J. (2008). Principles and Practice of Variable Pressure Environmental Scanning Electron Microscopy (VP-ESEM). Chichester: John Wiley & Sons. ISBN 978-0470758748.
- [23]. B. Aljafari, T. Alamro, M. K. Ram, A. Takshi, J. of Solid State Electrochemistry, (2019) 23:125-133.
- [24]. *J. Mater. Chem. A*, 2018,6, 18994-19003.
- [25]. XIA L, YU L, HU D, et al. Electrolytes for electrochemical energy storage [J]. *Materials Chemistry Frontiers*, 2017, 1(4): 584-618.
- [26]. *J. Mater. Chem. A*, 2015, 3, 7368.
- [27]. Zhou, M., Zhang, H., Qiao, Y. et al. *Cellulose* (2018) 25: 3459.  
<https://doi.org/10.1007/s10570-018-1786-3> PVA H3PO4
- [28]. Olakunle Alao, Paul Barendse, "Online Condition Monitoring of Sealed Lead Acid & Lithium Nickel-Cobalt-Manganese Oxide Batteries using Broadband Impedance Spectroscopy", Energy Conversion Congress and Exposition (ECCE) 2018 IEEE, pp. 2026-2032, 2018.
- [29]. Gamry Instruments, Testing Super-Capacitors, White Paper.
- [30]. Volume 49, Issue 24, 30 September 2004, Pages 4157-4161.
- [31]. Li, Saisai et al. "Preparation of Hierarchically Porous Graphitic Carbon Spheres and Their Applications in Supercapacitors and Dye Adsorption." *Nanomaterials* (Basel, Switzerland) vol. 8,8 625. 17 Aug. 2018, doi:10.3390/nano8080625
- [32]. Young Hwi Kwon *et al* 2018 *Nanotechnology* **29** 195404
- [33]. *J. Mater. Chem. A*, 2016, 4, 16213